



## Review article

Characteristic effects of alloying elements on  $\beta$  solidifying titanium aluminides: A reviewSadiq Abiola Raji<sup>a,d,\*</sup>, Abimbola Patricia Idowu Popoola<sup>a</sup>, Sisa Leslie Pityana<sup>a,b</sup>, Olawale Muhammed Popoola<sup>c</sup><sup>a</sup> Department of Chemical, Metallurgical and Materials Engineering, Tshwane University of Technology, Staatsartillerie Road, Pretoria West, Pretoria, South Africa<sup>b</sup> National Laser Centre, Council for Scientific and Industrial Research (NLC-CSIR), Meiring Naude Road, Pretoria, South Africa<sup>c</sup> Department of Electrical Engineering, Centre for Energy and Electric Power, Tshwane University of Technology, Staatsartillerie Road, Pretoria West, Pretoria, South Africa<sup>d</sup> Department of Metallurgical Engineering, Yaba College of Technology, P.M.B. 2011 Yaba, Lagos, Nigeria

## ARTICLE INFO

## Keywords:

Materials science  
Nanocomposites  
Metallurgy  
Alloys  
Composite materials  
Materials characterization  
Gamma-titanium aluminides ( $\gamma$ -TiAl)  
Microstructural formation in titanium aluminides  
Grain refinement  
Alloy development  
Effects of alloying elements  
Heat treatments of titanium alloys

## ABSTRACT

The high strength-to-weight ratio property of titanium aluminide (TiAl) based intermetallic alloys makes researchers regard this type of material as a potential replacement for the heavier superalloys of nickel. These alloys have been applied as turbocharger wheels of automobile and turbine blades of aircraft engines. A much recent alloy type of TiAl called the TNM alloy has emerged and primarily amenable to mechanical working; while providing the best combinations of mechanical properties that could be achieved through manufacturing processes with subsequent heat treatments. This is attained by solidifying entirely through the disordered  $\beta$ -phase (A2 structure). Effects of major alloying elements such as strength improvement, microstructural stability and phase formation demand the understanding of these alloying elements addition in TiAl-based intermetallic alloys. This review paper aims at encapsulating several works regarding the effects of major alloying elements on  $\beta$ -solidifying TiAl-based alloys and summarizing the characteristic effects of Si for these types of alloys. An impetus for future works on these types of intermetallic TiAl-based alloys is also presented.

## 1. Introduction

Recently, an innovative variety of beta-solidifying ( $\beta$ -solidifying) titanium aluminide (TiAl) alloys have been developed by several researchers dubbed TNM and TNM<sup>+</sup> alloys [1, 2, 3, 4, 5, 6]. In contrast to the peritectic solidification pattern prone to segregation, these alloys produce fine-grained homogeneous structures by solidifying entirely through the disordered  $\beta$ -phase (A2 structure) having a body-centred cubic (BCC) lattice structure [4, 7, 8, 9, 10, 11]. Oehring et al. [12], suggested the phase transformation pathway liquid  $\rightarrow \beta \rightarrow \beta + \alpha (-\alpha) \rightarrow \alpha + \gamma (+\beta) \rightarrow \alpha_2 + \gamma (+\beta)$  for  $\beta$ -solidifying alloy in achieving complete solidification. Also, Imayev et al. [8], realized that a TiAl-based alloy with 44 at.% Al content which contains boron (B) transforms through a solid-state solidification pathway as  $L \rightarrow L + \beta \rightarrow \beta \rightarrow \alpha + \beta \rightarrow \alpha \rightarrow \alpha + \gamma \rightarrow \alpha_2 + \gamma$ . While Tian et al. [13], observed that Ti-48Al-2Nb-2Cr (at.%) alloy (4822) has a transformation path based on phase diagram which follows  $L \rightarrow L + \beta \rightarrow L + \beta + \alpha \rightarrow \alpha \rightarrow \alpha + \gamma \rightarrow$  lamellae ( $\alpha_2 + \gamma$ ). All compositions are

presented in atomic percentage except stated otherwise. Cobbinah and Matizanhuka [14], stated that a typical TiAl alloy solidifies entirely via the single  $\alpha$ -phase region as  $\alpha \rightarrow \alpha + \gamma \rightarrow \alpha_2 + \gamma$  or  $\alpha \rightarrow \alpha_2 \rightarrow \alpha_2 + \gamma$ . It is understood that subject to the cooling rate and solidification path, distinct phase compositions and microstructures could be achieved. Hence, making it possible to control these microstructures in obtaining specific and desirable or peculiar material properties.

Apart from Ti and Al, TNM alloys contain alloying elements such as Nb, Mo and minor additions of B [8, 12, 15, 16, 17, 18]. This was developed primarily to be amenable to mechanical working while providing the best combinations of mechanical properties that could be achieved through manufacturing processes with subsequent heat treatments. TNM alloys are quite sensitive in varying the microstructural grain sizes, morphology and decomposition of lamellae depending on the alloying elements. Thus, the curiosity in understanding the microstructural evolution and phase compositions. At elevated temperatures, TNM alloys display satisfactory quantities of disordered  $\beta$ -phase because of the

\* Corresponding author.

E-mail addresses: [RajiSA@tut.ac.za](mailto:RajiSA@tut.ac.za), [rajisadiqa@gmail.com](mailto:rajisadiqa@gmail.com) (S.A. Raji).

$\beta$ -stabilizing effects that Mo and Nb offer in promoting hot-workability of TiAl-based alloys [7, 15, 16, 17, 18]. TNM alloys containing micro-alloys of Si and C called TNM<sup>+</sup> are said to demonstrate excellent creep resistance properties and exceeding the present service temperature limits for TiAl alloys [5]. This is a process-adapted alloy that allows for one-step heat treatment in the  $\alpha$ -phase region to attain microstructure of fully lamellar. Different cooling rates during annealing results in adjustments of the  $\alpha_2/\gamma$  colonies and lamellar spacings.

Furthermore, it must be noted that the detrimental effects of the  $\beta$ -phase at the material's service temperatures could be easily reduced and/or completely removed with appropriate heat treatment techniques [16, 19, 20]. This detrimental effect emanates from the disordered A2 structure transforming at ambient temperature to the ordered B2 structure ( $\beta_0$ -phase) which is brittle and harder than  $\gamma$  and  $\alpha_2$  phases. Also, the  $\beta_0$ -phase is incompatible with the  $\alpha_2$  (D0<sub>19</sub> structure) and  $\gamma$  (L1<sub>0</sub> structure) phases leading to crack nucleation and propagation at the  $\beta_0/\gamma$  interfaces, thereby, causing a reduction in ductility at the service temperatures [16, 20, 21, 22]. This crack initiation has a significant influence on the fracture of TNM alloys [22]. However, in the study of Cui et al. [19], it was observed that the  $\beta$ -phase was not detrimental to the room-temperature ductility. Microalloying elements additions of B, Si and C were added to act as nucleation agents in TNM alloys during solidification and phase transformations. Moreover, B has proven to be the most effective for grain refinement [8, 12, 23]; while C and Si were more suitable in improving the maximum operating temperatures of TNM alloys giving rise to a promising alloy subclass known as TNM<sup>+</sup> [1, 3, 4]. Another important phase (though it is minor) present in TNM alloys is the  $\omega_0$ -phase [7, 24]. This phase is barely identified through a scanning electron microscope (SEM) because the phase has a fine nature that is mostly observed as precipitates in the  $\beta_0$ -phases [24, 25]. The specific nature of occurrence and mechanism of its precipitation reactions are still not fully understood and it is still an ongoing discussion of research between scientists.

At room temperature, TiAl intermetallic alloys comprise of three major phases of intermetallics, namely;  $\alpha_2$ -Ti<sub>3</sub>Al (D0<sub>19</sub> structure),  $\gamma$ -TiAl (L1<sub>0</sub> structure) and  $\beta_0$ -TiAl (B2 structure) [1, 4, 7, 18, 20, 26, 27, 28, 29]. The  $\gamma$ -TiAl phase has L1<sub>0</sub> tetragonal structure while  $\alpha_2$ -Ti<sub>3</sub>Al phase has a D0<sub>19</sub> hexagonal structure [30, 31, 32, 33, 34]. Also, the  $\gamma$ -TiAl phase is formed at 49 to 66 at.% Al content [14] that could be stabilized up to its melting temperature (~1450 °C) [28]. It possesses high specific modulus, low density, good oxidation resistance, excellent fatigue, and creep properties [35]. The  $\gamma$ -phase (L1<sub>0</sub>) of lattice parameters  $a = 0.4005$  nm and  $c = 0.4070$  nm has an ordered face centred tetragonal (FCT) structure [14, 34] and transforms to the disordered structure at about 1250 °C [29]. The ordered  $\gamma$ -phase has low ductility (up to 750 °C), thereby, decreases its plastic deformation capability likewise does the ordered  $\alpha_2$ -phase have low ductility (up to 600 °C) [30]. This is because of the limited number of slip systems, the occurrence of planar slip [30, 36] and lack of twinning [32] which makes these phases brittle.

The  $\alpha_2$ -Ti<sub>3</sub>Al phase has an ordered hexagonal closed packed (HCP) structure [33, 34] formed between 22 to 39 at.% Al content and transforms to an ordered structure from the disordered one at about 1180 °C with lattice parameters,  $a = 0.5782$  nm and  $c = 0.4629$  nm [14, 34]. It is known to exhibit extremely poor toughness and tensile ductility at ambient temperatures while possessing good oxidation resistance and excellent elevated temperature specific strength [28]. Typical TiAl-based alloy microstructures consist of alternating  $\alpha_2/\gamma$  lamellae formed within the  $\alpha$ -phase region and present a reciprocating crystallographic relationship of (0001)- $\alpha_2$  || (111)- $\gamma$  and  $\langle 1120 \rangle$ - $\alpha_2$  ||  $\langle 110 \rangle$ - $\gamma$  [34, 37]. The principal modes of deformation in  $\gamma$ -phase are  $\langle 110 \rangle$  slip and  $\{111\} \langle 112 \rangle$  twinning while  $\alpha_2$ -phases is between the  $\gamma$  twinned phases [34]. The high Al content of the  $\gamma$ -phase makes it achieve higher resistance against oxidation than  $\alpha_2$ -phase [38]. Jian et al. [39], reported that the  $\alpha_2$ -phase shows strong metallic bond with low mechanical anisotropy; while  $\gamma$ -phase has a covalent bond with strong universal mechanical anisotropy. It is commonly known that to maintain the ordered D0<sub>19</sub>

structure, a large interchange shuffling is required [32, 40]. The appearance of  $\alpha_2$ -phase deformation twinning could play a key role in high Nb-containing TNM alloys' mechanical properties enhancement. This will help in understanding and further the development of  $\beta$ -solidifying  $\gamma$ -TiAl-based alloys. Furthermore,  $\beta_0$ -phase has a body-centred cubic (BCC) structure which is similar to conventional  $\beta$ -phase Ti alloys with B2 superlattice structure [33]. As stated earlier, the disordered elevated temperature  $\beta$ -phase changes to a very brittle and hard  $\beta_0$ -phase at room temperature (RT) [16]; while ordered  $\beta_0$ -phase dissolving to disordered  $\beta$ -phase at about 1175–1205 °C [29]. In typical Ti alloys, there are both high-temperature BCC  $\beta$ -phase and low-temperature HCP  $\alpha$ -phase [41].

It was reported by Jiang et al. [28], that addition of Nb as BCC  $\beta$ -stabilizer in both  $\alpha_2$ -Ti<sub>3</sub>Al and  $\gamma$ -TiAl contributed to the development of ordered B2-Ti(Al, Nb) or orthorhombic O-Ti<sub>2</sub>AlNb phases. Besides, Nb and Mo as  $\beta$ -stabilizing elements are added in TiAl-based alloys to enhance RT ductility through the formation of minor  $\beta$ /B2 phase quantities [28]. It is well reported in literature that  $\beta$ -stabilizing elements such as Mo, V, Ta, Nb, Mn, Zr and Cr are favoured to enter the Ti sites. Moreover, the addition of  $\beta$ -stabilizers into  $\beta$ -Ti inhibits  $\beta$ -Ti  $\rightarrow$   $\alpha$ -Ti transformation that leads to intermediate  $\omega$ -Ti phase formation (hP-AlB<sub>2</sub> type) [28].

According to Singh et al. [31], TiAl intermetallic alloys lack hot-workability due to reasons such as (i) low dislocation mobility, (ii) shortage of independent slip system resulting in the materials' plastic anisotropy, and (ii) lack of mobility at grain boundaries and diffusivity caused by retarded recrystallization and recovery. Also, the practical application of TiAl alloys is inhibited by poor oxidation at elevated temperatures [42]. Titanium aluminides are problematic to process due to their brittle nature, hence, limiting its widespread production. The intrinsic brittleness at RT and poor hot-deformability limit its application in manufacturing complex-shaped structural components [14, 31, 39, 42, 43, 44, 45, 46, 47, 48]. Consequently, conventional processing of TiAl-based alloys such as forging and extrusion are restricted; while casting is known to always produce coarse microstructure and arbitrary defects resulting in inhomogeneous mechanical properties [20, 47]. This is caused by high strain at elevated temperatures and poor RT ductility of TiAl-based alloys.

However, several heat treatment procedures and/or mechanical processing routes have been exploited based on the transformation of phases in manipulating the resultant microstructures. These processing techniques allows for a balance in desirable properties while gaining control of the colony sizes, lamellar spacing, grain size and grain growth. Chen and Li [30], reported that ordered structures of TiAl-based alloys and their morphological texture causes mechanical properties inhomogeneity. Four possible microstructures are usually formed by TiAl-based intermetallic alloys are shown in Figure 1. It is reported that the nearly fully lamellar and/or fully lamellar microstructures could provide the much-needed combination of mechanical properties using a viable production method and provide structural integrity during the components' lifetime [5, 7, 14, 16, 22, 30, 46, 51, 52]. The duplex or equiaxed microstructure ( $\gamma + \alpha_2$ ) provides adequate ductility and fatigue but it exhibits low creep resistant and fracture toughness; while the microstructure with fully lamellar (with alternating plates of  $\gamma$  and  $\alpha_2$  phases) demonstrates superior fracture toughness and creep resistant but demonstrates poor ductility [30, 31, 52]. Hence, the choice of final microstructure during processing is very essential to obtain the best combination of mechanical properties. This is because of the transpose correlation between fracture toughness and ductility in the different microstructures. To further understand these microstructures, the reader could read refs [14, 48, 49, 50].

The gamma-TiAl ( $\gamma$ -TiAl) alloy is a novel type of lightweight material [53].  $\gamma$ -TiAl-based alloys are potential substitutes for nickel (Ni) based superalloys especially in applications that require considerable weight saving and minimal redesigning [15, 28, 48, 54, 55, 56, 57, 58, 59, 60, 61, 62]. According to Ding et al. [63],  $\gamma$ -TiAl alloys with FL

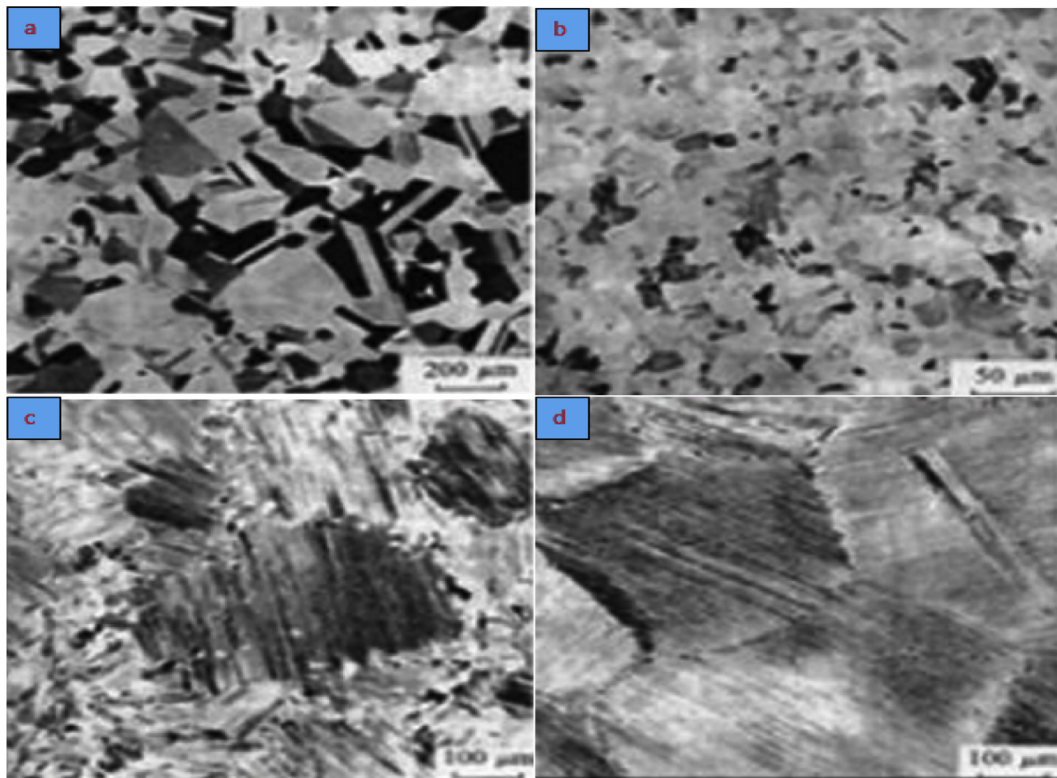


**Figure 1.** Typical phases of TiAl-Based Alloys; (a) Equiaxed or Near Gamma (NG or near  $\gamma$ ) (b) Duplex Phase (DP) (c) Near Lamellar (NL) (d) Fully Lamellar (FL) [49, 50].

microstructures creates decent stability in properties such as ductility, creep resistance and fatigue resistance which are often needed in several engineering applications.  $\gamma$ -TiAl alloys serve as a feasible substitute in aircraft engine applications for turbine blades and turbochargers wheels. However, oxidation resistance above 800 °C is another major drawback in expanding its usage in high-temperature applications [64].

Previous works have shown that enhance mechanical properties could be achieved by the dual-phase ( $\alpha_2/\gamma$ ) alloys. Particularly, lamellar microstructures in respect of fracture toughness, higher strength and ductility when compared to either the single phases of  $\gamma$  or  $\alpha_2$ . The duplex and fully lamellar are the two most common microstructures of TiAl-based alloys for engineering applications. The  $\alpha_2$  and  $\gamma$  phases display diverse behaviours during deformation owing to their distinctive crystal structures [63]. The Blackburn orientation relationship (BOR) expresses the crystallographic relationship between these phases [37, 65]. A semi-coherent interface would result from any slight difference in the lattice parameters of both  $\gamma$  and  $\alpha_2$  phases. The transfer of dislocations from one phase to the other is difficult because  $\alpha_2$ -phase is a very brittle phase; thus, reducing the overall ductility in fully lamellar microstructures [31].

This has made researchers study the fundamental phenomenon in understanding the  $\alpha_2$ -phase of the dual-phase alloys which retains the highest levels of O impurity [59, 66, 67, 68]. Ren et al. [68], explained that microhardness and nano-indentation measurements revealed that significant precipitation hardening arises in  $\gamma/(\alpha_2+O)$  lamellar due to O phase present in  $\alpha_2$  lamellae. This is attributed to the refinement of  $\alpha_2$  lamellae in relation to the interface and phase transformation. This is because the elastic strain energy introduced between the adjacent  $\gamma$ -phase and modulated lamellae. This is also because of the thermodynamic equilibrium of O phase and retention of a high-volume fraction within the  $\alpha_2$ -phase. Hence, it is critical to control the microstructure and ensuing mechanical properties in producing a high-performance  $\beta$ -solidifying  $\gamma$ -TiAl alloy [68]. However, there are divergent views by researchers regarding the so-called “scavenging effect” stating that the

$\gamma$ -phase is ductile compared to  $\alpha_2$ -phases. The precipitation of fine-scaled oxides owing to excess O results in embrittlement because the solubility of O in the  $\gamma$ -phase of TiAl alloys is limited [7, 69]. Lefebvre et al. [69], maintained that O, C or N have a preference to dwell in the  $Ti_6$  octahedral sites which are situated in  $\alpha_2$ -phase. Moreover, if the composition of phases in  $\gamma$  changes to the Al-lean area of the stoichiometric composition, the excess Ti atoms occupy Al sites resulting in cavity formation of  $Ti_6$  octahedral. Other researchers like [24, 25, 50], used this conclusion to explain their observations of Nb, stating that excess Ti is generated as Ti is favourably substituted in the  $\gamma$ -phase by the Nb atoms that locate the Al sites. Thereby, raising the concentration of  $Ti_6$  octahedral site which acts unvaryingly to off-stoichiometry.

Titanium aluminides are potential engineering materials where lightweight is required including strength retention at elevated temperatures [65]. Due to a density between 3.8 to 4.3 g/cm<sup>3</sup>, TiAl-based alloys are ideal candidates in aircraft applications [16, 19, 35, 64]. For the past three decades, titanium aluminides intermetallic alloys have been of major interests especially in the aerospace and automotive industries. This is essentially due to their attractive mechanical properties like high strength-to-weight, low density, excellent high-temperatures stiffness and strength retention [15, 28, 31, 43, 46, 47, 48, 50, 56, 62, 67, 69, 70, 71, 72, 73, 74, 75, 76, 77, 78, 79, 80]. This makes TiAl-based alloys a type of material with very high prospects of replacing nickel-based superalloys typically used for making aircraft-engine turbine parts [43]. However, poor hot workability is a major problem concerning TiAl alloy.

The intermetallic Ti–Al ordered system is still a topic of extensive study because of its inherent applications for structural materials operating at elevated temperatures [6, 23, 47, 53, 54, 60, 69, 79, 80, 81, 82, 83, 84, 85, 86]. The successful integration of TiAl-based alloys parts into aircraft engines is predicted to tremendously decrease greenhouse gas emission and fuel consumption [5]. Thus, titanium aluminide has found application in making seal supports, cases and frames of aircraft engines where clearances are crucial [54]. Also, it is applied in turbocharger wheels and turbine blades of automobile and aero engines respectively

[5, 7, 21, 43, 50, 58, 73, 79, 80, 81, 87, 88, 90, 91]. Considerable decrease in fuel consumption and greenhouse gases have been achieved due to the lightweight of rotating components. Moreover, fracture toughness and limited ductility at RT hampers the widespread applications of TiAl-based alloys in fabricating functional parts [8, 15, 26, 73]. This could be overcome by micro-alloying elements additions [15, 51]. Also, crack initiation and propagation, inferior performance in hot oxidizing atmospheres (above 750 °C) and low fatigue life are the main problems hindering its wider adaptability as aero-engine components [18]. Mengis, Grimme and Galez [92], stated that high-temperature wear is also a major concern for turbine engines.

Moreover, lots of work have been carried out by several researchers using different processing techniques in developing suitable microstructures with compositions. Recently, TiAl has become a well-known class of material with established processing routes which is an indication of increased market penetration in both aerospace and automobile industries [7]. Pratt & Whitney have applied TiAl in producing low-pressure turbine (LPT) blades for their PW1100G turbofan engine; while general electric (GE) developed the LEAP-1A Safran aircraft engines from TiAl alloy [81]. The Ti-48Al-2Nb-2Cr (4822 alloy) has been adopted by general electric (GE) to manufacture their LPT blades in Boeing 787 and 747-8 of GENx engines [15, 64, 93]; while Ti-43.5Al-4Nb-1Mo-0.1B (TNM) alloy was used for LPT stage of GTF engine by Pratt and Whitney [15]. Also, Ti-46.5Al-3.5Nb-2Cr-0.3B alloy is used to make wrought turbine blades [94]. Owing to their attractive stiffness, vibration frequencies are shifted upward that is typically advantageous in structural parts [54]. The use of Ti-Al alloying systems in these engines has resulted in decreasing 20% fuel consumption, 80% NOx emissions and 50% operation noise of the GENx engines, compared to similar engines [83].

According to Castellanos et al. [77], most machinability research studies agree that the poor machinability of TiAl-based alloys is due to (a) the formation of surface cracking, shear bands and vibration waves that are catastrophic to the workpiece surface; (b) the shortened tool service lifetime and poor surface integrity when cutting at high-temperatures; (c) the tooltip and high thermal gradient generated at high temperatures because of poor thermal diffusivity of TiAl alloys; (d) the tendency of material hardening during machining causes notch wear of the tool; and (e) the adhesion of the tool to the cutting edge owing to high chemical affinity. The transformation caused by machining on the surfaces of workpiece leads to poor quality of the machined component and shortens the tool's lifespan. Tools' producers and researchers are faced with the difficulties arising from the poor machinability of TiAl-based alloys. Castellanos et al. [77], reported that cracks are produced at the  $\gamma$ - $\gamma$  lamellae interfaces of  $\gamma$ -TiAl and poor ductility hinders the realization of defect-free surfaces. The major defects during machining operations on TiAl alloy surfaces reported in literature are work-hardening tendencies, surface cavities, smearing, feed marks, lamellar deformation, cracking and material pull-out [77, 83]. Due to the plastic deformation, sub-surface microstructures are altered during machining of bulk materials. The consensus of opinions on milling and turning operations for work-hardening is that the hardness of machined workpiece increases as the depth and feeding value increases on the material surface. Furthermore, abrasive wear is known to be the foremost mode of failure during machining of TiAl-based alloys because of the work-hardened layer.

It is commonly agreed that some alloying elements can effectively increase the stability of microstructures and consequently improve creep resistance with other mechanical properties. This may be attributed to reduced interface mobility due to interfacial segregation. This paper presents an overview of the development of  $\beta$ -solidifying  $\gamma$ -TiAl intermetallic alloys produced using different microalloying elements and/or combination of various heat treatment procedures with the phase transformations and final microstructures produced to achieve certain mechanical properties. The main objective of this review paper is to analyse scientific works on the influence of some alloying elements on

$\beta$ -solidifying intermetallic TiAl-based alloys with succinct behaviour of Si on this type of alloy.

## 2. Effects of alloying elements on TiAl-Based alloys

This section discusses the influence of well-known alloying elements effects that are characteristically used in developing superior titanium aluminide intermetallic alloys. According to Fang et al. [45], the benefits of alloying are to (i) cause relaxation of slip modes restriction; (ii) reduce the ordering kinetics or alter long-range ordering degrees; (iii) modify the alloy structure by introducing  $\beta$ -phase as a ductile phase to mitigate microcrack growths formed in  $\alpha_2/\gamma$  phases; (iv) adjust transformation behaviour when processing or heat treating to facilitate the control of microstructural refinement. It is understood that Al contents are central to manipulating the microstructural transformations, phase evolution and lamellar content ( $\alpha_2+\gamma$  phases) in TiAl-based alloys.

In  $\beta$ -solidifying  $\gamma$ -TiAl-based alloys, alloying elements aimed at improving the mechanical properties include Nb, Mo, V, Cr and Mn for increasing ductility and stabilizing  $\beta$ -phase in the microstructure [45, 57, 95]. Others include Ta, Mo and W that are meant to improve oxidation resistance [45]; while B, C and Si are for microstructural refinement [45, 93]. Among these alloying elements, effective hardening is caused by C when finely dispersed precipitates of carbides are formed in TiAl-based alloys. According to Ye et al. [59],  $\beta$ -stabilizing effects or  $\beta$ -phase stability of alloying elements are commonly measured by the valency of electrons per atom (i.e. electron concentration). Stronger  $\beta$ -stabilizing effects are easily noticed by alloying elements with more valence electrons. V tends to show stronger  $\beta$ -stabilizing effects than Nb and Ta, though V, Nb and Ta contain similar valency of electrons; likewise, does Cr over Mo and W [59]. Hence, the  $\beta$ -stabilizing effects are not only measured by the number of valence electrons. Ye et al. [59], reported that the volume per unit of atoms in the system could also influence  $\beta$ -stabilizing effects. It was stated that alloying elements with a smaller atomic radius such as Mn, V, and Cr leads to a higher density of valence electrons and lower volume per unit atoms, thereby, resulting in more stable  $\beta$ -phase formation.

### 2.1. Phase formation and microstructural stability

Transition metals like V, Nb, Ta, Mo, Cr, Mn and W are common and important alloy additions of TiAl-based alloys for improving mechanical properties especially their fracture toughness and ductility at RT. This is usually achieved by deliberate microstructural alterations with slip and twin deformation of solute elements [34]. The addition of the  $\beta$ -stabilizing elements also causes grain refinement by changing the solidification pathway and formation of  $\beta$ -phase to enhance the workability of TiAl-based alloys [35]. Moreover, in understanding TNM alloys and related alloys, the effects of Mo and Nb are distinctively essential, because they are usually present as major alloying constituents [4, 7, 12, 15, 18, 24, 26].

In a study by Kainuma et al. [96], it was concluded that W, Ta, Mo, Cr and V partitions  $\alpha_2$  or  $\alpha$  phase at the  $\alpha/\gamma$  and  $\alpha_2/\gamma$  phase equilibria while Zr does same in the  $\gamma$ -phase; but Nb, Cu, Ni, Co, Fe and Mn changes to  $\alpha$  formers from  $\gamma$  formers as temperature increases. These phenomena of alterations in partitioning behaviour were attributed to the FCC and HCP lattice structural stability difference between the alloying elements. However, for the phase equilibria ( $\beta/\alpha_2$ ,  $\beta/\alpha$ , and  $\beta/\gamma$ ) only Zr partitions the  $\beta$ -phase, unlike other elements partitioning at the  $\gamma$ ,  $\alpha_2$  or  $\alpha$  phases. According to Kainuma et al. [96], the partitioning tendency at  $\beta/\alpha$  equilibria is largely dependent on the interfacial energy between the HCP and BCC lattice structures in Ti-X (X = V, W, Nb, Co, Fe, Ta, Mo, Cu, Ni, Cr, Zr) binary systems. Bresler et al. [65], showed that domain boundaries and interfaces of  $\gamma/\gamma$  phases diminishes the movement of dislocations and plastic deformation but not like the  $\alpha_2/\gamma$  interface. Since the  $\gamma$  and  $\alpha_2$  phases exhibit different slip systems, the movement of dislocations is restrained when compared to the  $\gamma/\gamma$ -interfaces. Hence, the mean



spacing between the interfaces of  $\alpha_2/\gamma$  affects the creep properties of TiAl alloys but not the colony boundaries and sizes. It has also been recognised that alternating microstructures of  $\alpha_2+\gamma$  lamellar leads to better resistance to creep in comparison to the equiaxed microstructures [54, 74]. This is related to the strong anisotropy of lath structures and large grain sizes, thus, high brittle-ductile-transition-temperature (BDTT) [74, 81]. Likewise, an increase in  $\alpha_2$ -phase and structural refinements is known to cause strengthening effects in the dual-phase  $\alpha_2+\gamma$  TiAl intermetallic alloys [50, 74].

Niobium (Nb) addition in  $\gamma$ -TiAl-based alloys stands out when compared to most alloying elements in providing a balance elevated temperature and RT properties [14]. These mechanical properties enhancement is ascribed to the combined influence of precipitation strengthening, solid solution strengthening, increase in  $\gamma$ -phase content and grain boundary strengthening [45]. It is well reported in literature that Nb plays a vital role in oxidation resistance and high-temperature strength improvements in TiAl-based alloys [15, 18, 25, 97]. Nb favours Al activities and prefers the formation of  $\text{Al}_2\text{O}_3$  which act as a protective oxide surface, thereby, limiting oxygen diffusion into the alloy [55]. These positive effects of Nb manifest through increased propensity of the  $\alpha_2$ -phase basal slip, ductile  $\beta$ -phase stabilization, and oxidation resistance improvement [35, 55]. This is related to the Nb solid solubility which increases within the  $\gamma$ -phase and lesser diffusion in  $\alpha_2$ -phase; while segregation of Nb results in B2-phase formation [45]. The B2-phase is formed through a  $\beta$ -phase transformation and  $\alpha$ -grains nucleation in the  $\beta$ -grains. Refinement of lamellar colonies and heterogeneous nucleation sites formation is promoted by the addition of Nb.

Nb being a  $\beta$ -stabilizer cause the retention of  $\beta_0$ -phase at ambient temperatures, particularly for  $\beta$ -solidifying TiAl-based alloys. The  $\beta_0$ -phase is an ordered derivative of the disordered  $\beta$ -phase retained at RT [97]. Consequently, microstructural inhomogeneities as a result of strong partitioning lead to reduced fatigue and creep resistance. This is expected due to considerable difference of Nb distribution in the phases in comparison to the traditional dual-phase TiAl-based alloys [7, 97]. In TiAl-based alloys with high Nb content, the emergence of  $\beta_0$ -phase leads to reduced RT ductility and the formation of  $\omega$ -phase from the parent  $\beta_0$ -phases. The  $\omega'$ ,  $\omega_0$  and  $\omega$  (D8<sub>8</sub> structure) phases occur at separate stages during the  $\beta_0 \rightarrow \omega_0$  or  $\beta_0 \rightarrow \text{D8}_8\text{-}\omega$  transformations [25, 40, 97]. Depending on the cooling methods adopted, the  $\omega$ -related phases vary in morphology, size, and structure around the  $\beta_0$ -phases [24]. Nb addition in TiAl-based alloys enhance the oxidation resistance, toughness at RT and creep resistance. Nonetheless, high amount of Nb would densify the alloy, thereby, limiting the alloy applications [10, 72, 95]. It has been observed that the composition of Al and Ti in  $\beta_0$  and  $\alpha_2$  phases are in contrast with what is obtained in the  $\gamma$ -TiAl and  $\alpha_2$ -Ti<sub>3</sub>Al binary phases [9]. The different sites occupied by these metal atoms in the alloy causes this nonconformity. It was also reported from ab initio calculation of refs [2, 26], that transition metal atoms favours substitution of both Al and Ti sites in  $\beta_0$  and  $\alpha_2$  phases respectively, showing stronger tendencies in the latter. Generally, Nb demonstrates a weak preference for the  $\beta_0$ -phase but shows almost the same amount of distribution in other phase confirming Nb as a  $\beta$ -stabilizer in TiAl-based alloy systems [7].

Doping of Ti–Al binary system with Mo promote a rise in ionic or covalent bonds resulting in improved elasticity modulus and strength [98]. Based on the observations from literature [12, 24, 81, 99], Nb addition in TiAl-based alloys still retains substantial quantities of Nb in other phases even with the initiation of the  $\beta_0$ -phases that are quite stable at ambient temperatures. However, Mo still favours the formation of more  $\beta_0$ -phase but behaves differently by creating strong partitioning between phases. This is because Mo is a stronger  $\beta$ -stabilizer compared to Nb and broadly influences processing, which has been well reported by refs [9, 15, 24, 81, 94]. Also, hot-working is achievable using near conventional equipment because the disordered  $\beta$ -phase is stabilized at elevated temperatures with small additions of Mo [26, 82, 94, 100]. Moreover, heat treatment could be applied to decrease the  $\beta/\beta_0$  volume fraction due to the detrimental creep resistance effects [24, 99, 100]. The

ordered  $\beta_0$ -phase with A2 structure is reported to have high energy of formation, thus, making it more stable chemically when compared to the disordered  $\beta$ -phase having a B2 structure. However, the disordered  $\beta$ -phase has better mechanical stability than  $\beta_0$ -phase [26]. Erdelyi et al. [9], investigated the precipitation behaviour of the  $\gamma$ -phase growth in a Ti–44Al–7Mo  $\beta$ -homogenised alloy within the supersaturated  $\beta_0$ -matrix. The results showed that the transformation of  $\beta_0 \rightarrow \gamma$  phase occurred without forming any intermediate phase with diverse crystallographic structures. This  $\beta$  single-phase homogenisation treatment triggers the dissolution of  $\alpha_2$  and  $\gamma$ . Subsequently, water quenching (WQ) invariably subdued the re-precipitation of  $\alpha/\alpha_2$  and  $\gamma$  which prevents martensitic or massive transformation. Thus,  $\beta_0$  single-phase microstructure is preserved at RT.

Several authors [4, 9, 24, 26, 61, 80, 81, 82, 83, 84, 85, 86, 87, 88, 89, 90, 91, 100, 101, 102] have used a dual-stage heat treatment process in trying to reduce the  $\beta$ -phase. These TiAl-based alloys were first heated to a temperature above the  $\gamma$  solvus temperature ( $T_{\gamma\text{solv}}$ ), held for a brief period to avoid grain growth with subsequent fast cooling. While the second heat treatment was conducted at a temperature higher than the predicted service temperature, held for a prolonged period followed by slow cooling (or furnace cooling). This is done because Mo barely stabilizes the ordered  $\beta_0$ -phase but effectively stabilizes the disordered  $\beta$ -phase. In comparison to Ti and Al, Mo seems rather slow in diffusing the B2 structure. This is because the self-diffusion energies of Al and Ti for short distance diffusions are lower than the activation energy of Mo in the alloy [9]. Also, it results in phase fraction equilibria and regulated fine lamellar microstructure leading to phase transformation and improved oxidation resistance. Impurities observed in TiAl-alloys are most prevalent in the  $\alpha_2$ -phase as an interstitial element. This impurity dissolves in the  $\alpha_2$ -phase because of the Ti<sub>6</sub> octahedral sites which favour the incorporation of these interstices [7]. The  $\gamma$  and  $\beta$  phases do not possess or contain any octahedral sites. According to Erdelyi et al. [9], the rationalization of diffusion role in the  $\gamma$ -phase formation at equilibrium is considered that: (i) partition of elements must take place between the phases, and (ii) owing to energetic reasons, atoms of Mo must relocate to the Ti sublattice in  $\gamma$  from the Al sublattice in  $\beta_0$ . Consequently, it could be said that the redistribution elements instead of interfacial migration governs the growth of diffusion precipitates in the  $\gamma$ -phase.

In the work of Cui et al. [19], it was noticed that the difference in hardness between the  $\beta$  and  $\gamma$  phases was close. It was used to explain the lower hardness value recorded for  $\beta$ -phase which contributes to the superior tensile properties (RT elongation of about 1.5%) of Ti–43Al–2Cr–0.7Mo–0.1Y alloy with satisfactory hot-workability owing to high  $\beta$ -phase present. Moreover, the hardness values of TiAl-based alloys depend on the  $\beta$ -stabilizers and amount  $\beta$ -phase formed. It was also reported by Cui et al. [19], that alloys produced by Cr, Mn, and V had  $\beta$ -phase with low hardness; while Nb, Mo, or W resulted in  $\beta$ -phase of higher hardness values. The Reduction of hardness through alloying could be employed in designing compositions of  $\beta$ -solidifying TiAl-based alloys with excellent RT ductility.

Elements of zirconium (Zr) and Ti have the same atomic size and crystal structure belonging to group iv in the periodic table. Zr is said to refine TiAl-based alloy microstructures by dissolving completely in Ti within the  $\beta$ -phase region at elevated-temperatures and the  $\alpha$ -phase region at ambient temperature [103]. Zr occupies the Ti sites in the crystal lattice of TiAl-based alloys like  $\beta$ -stabilising elements of Mo and Nb [102]. The combined addition of Zr and Cr in TNM alloys promotes  $\omega$ -phase formation by increasing  $\beta$ -phase and decreasing the amount of  $\alpha_2$ -phase [104]. It was also reported that Zr improves compressive strength [104], enhances fracture strain and yield stress at intermediate temperatures [65]. It has been reported that diffusion of Zr is much faster than Nb and consequently it has little benefit in retarding diffusion-controlled processes.

Bresler et al. [65], investigated the influence of Zr, Nb and Ta on the creep properties of Ti–44Al–5X (X = Zr, Ta, Nb) ternary alloy. The microstructure was reported to be fully lamellar microstructure. All three

alloying elements were said to be highly soluble in the Ti–Al system and showed different  $\alpha_2/\gamma$  partitioning behaviour along with distinctive  $\alpha_2$  and  $\gamma$  phases lattice parameters. The atomic size difference and partitioning behaviour meant that the mean lattice parameter transformation misfits of  $\alpha_2/\gamma$  occur by the addition of microalloying elements [65]. Ta and Nb increase the misfit of  $\alpha_2/\gamma$  lattice, but Zr reduces it. Thus, the lesser the misfits of the lattices and coherent stresses, the more the dislocation emission decreases at the interfaces. According to Kainuma et al. [96], Nb partitioning is almost the same on both phases; while Ta partitioning occurs mainly at the  $\alpha_2$ -phase and largely at  $\gamma$ -phase for Zr which was also reported by Bresler et al. [65]. Microalloying and the rate of cooling has a substantial effect on the average distance of  $\alpha_2/\gamma$ -interfaces. It is understood that Zr and Ta show greater Nb segregation and the average spacing between the cores of dendrites were much smaller in the Ta-containing alloys compared to Zr- and Nb-containing alloys. The alloy (Ti–44Al–5Nb) had the least resistance to creep, whereas Ti–44Al–5Zr and Ti–44Al–5Ta exhibited almost the same creep resistance. Thus, it could be deduced that both Zr and Ta had enhanced creep resistance properties than Nb. It was proposed that due to the interfacial segregation of alloying elements and decelerating  $\alpha_2$ -phase dissolution during creep exposure. The slower kinetics of dissolution, rise in phase stability or decreasing misfits in lattices could be responsible for the Nb, Ta and Zr  $\alpha_2$ -stabilizing effects.

Ta as an alloying element is also used in TiAl-based alloys, but not often as Nb. As stated earlier, Ta enriches the  $\alpha_2$ -phase, Zr enriches the  $\gamma$ -phase whereas Nb equally partitions between both phases. The strong solid solution hardening effect and high solubility of Zr in the  $\gamma$ -phase are attributed to the exceptional creep properties of the TiAl alloy containing Zr; while interdiffusion coefficient of Ta is responsible for the Ta-containing alloy [65]. Ta can equally substitute Nb since the positions of Ta in the periodic table suggests they both would exhibit similar chemical behaviours. Likewise, high melting point of Ta makes it offer prospects of increasing TiAl-based alloys' operating temperature [20, 36, 55]. Research works on the effects of Ta in the TiAl-based alloys are usually on improving oxidation resistance. In trying to achieve the replacement of Nb with Ta, Cobbinah et al. [55], investigated the influence of adding Ta (0.8, 4 and 8 at.%) in Ti–46.5Al alloy produced by spark plasma sintered (SPS). The Ta-containing alloys showed the tendency of suppressing TiO<sub>2</sub> film growth while favouring the formation and growth of Al<sub>2</sub>O<sub>3</sub> by retarding the diffusion of oxygen; thus, inhibiting internal oxidation. It was explained that Ta creates doping effects, whereby, dopant element (like Ta) additions having a valency of +5 which are greater than valency of Ti (+4) leads to reduced defect concentration because of oxide electroneutrality realization.

In an experiment conducted to examine the correlation between microstructure and addition of Ta to produce B2-phase within the lamellar colonies, Fang et al. [36], prepared Ti46Al8Nb2.6CxTa alloys (Ta = 0–1.0 at.%) through casting. It was observed in the lamellar colonies that B2-phase formation increases with increased Ta content. This was reported to be favourable for microstructural control and modification. Ti46Al8Nb2.6C alloys with 0.8 and 1.0 Ta, offered the requirement needed for increasing the  $\alpha_2$ -phase and creating lamellar colonies with B2-phase. Moreover, the  $\alpha_2$ -phase lattice parameter increases, but that of  $\gamma$ -phase decreases. This is because Ta hinders the dispersion of Nb atoms from dissolving further within the lamellar colonies.

Furthermore, Ta is described to refine lamellar colony sizes of TiAl alloys [36]. This was attributed to the heterogeneous nucleation particles formed due to Ta additions. In related work, Fang et al. [20], investigated the mechanical properties of Ti42Al6Nb2.6C alloy produced by vacuum arc melting. It was noticed that above 0.2 at.% of Ta, the B2-phase seem to have vanished. This is ascribed to slow diffusion rate and the higher melting point of Ta, thereby, inhibiting Nb atom diffusion during solidification. This causes the disappearance of the B2-phase. The compressive strain and strength increase by 2.2 and 1.2 times, respectively, as Ta increases. There was an increment of 405 MPa–472 MPa for the tensile strength and 2.3%–2.9% for the strain as Ta increases at 750 °C. The

mechanical properties enhancement was due to the disappearance of the B2-phase and strengthening through Ta and Nb solid solutions [20]. Based on previous works, Ta and Nb display equal outstanding solubility in  $\alpha_2$  and  $\gamma$  phases. With additional solutes in  $\gamma$ -phase by the Nb atoms, more solutes of Ta are observed in the  $\alpha_2$ -phase. Zhang et al. [105], examined the formation of  $\gamma$ -phase in Ti–48Al–3Nb alloy with 0.5 at.% Ta after fast cooling from elevated temperature  $\alpha$ -phase region. A massive transformation was observed due to rapid cooling which displays sub-grains in  $\gamma_m$ -phase and fine nano-grain compared to retained  $\alpha_2$ -phase favoured in the Ti–48Al–3Nb alloy. It was reported that the solute atoms slow down the transformation of  $\gamma_m$ -phase during rapid cooling, which was analogous to the observation of other works in ref [20, 36, 55, 65].

Saedipour, Kermanpur and Sadeghi [52], examined the high-temperature mechanical properties and microstructural refinements of a Ti–46Al–8Ta alloy fabricated via vacuum arc re-melting with N addition up to 2 (at.%). The results presented demonstrated that N affects the as-cast alloys microstructure morphology, changes the transformation pathway, and caused notable microstructural refinement. From the viewpoint of thermodynamics, the solubility limit was exceeded by the N content leading to the formation of Ti<sub>2</sub>AlN. Furthermore, N extends the  $\alpha$ -phase field and up to 2 at.% addition does not affect the orientation relationship of  $\alpha_2$  and  $\gamma$  lamellae.

Influence of V and B was studied by Liu et al. [17] on the microstructural development of Ti–44Al–5Nb–1Mo–(B, V) alloy. Morphologies of dissimilar clubbed, granular, and chain-like primary particles were noticed in Ti–44Al–5Nb–1Mo–2V–0.2B alloys. The spacing size of lamellar increases in the alloys after hot isostatic pressing (HIP) as the alloying content increases. Also, the colony boundary sizes of B2 and  $\gamma$  grains increases. Besides, the degree of decomposition by the lamellar colonies increases the spacing of lamellar, and grain growth of B2 and  $\gamma$  as alloying elements are added. Ti–44Al–5Nb–1Mo alloy exhibited superior ultimate tensile strength (UTS) due to the fracture mechanism of inter-granular and trans-lamellar matched with a small fracture of micro-voids.

According to Tabie et al. [103], the addition of Sn as an alloying element in TiAl-based alloys is primarily applied in combination with Zr and Al to offer higher strength solid-solution strengthening without embrittlement. Addition of Sn can increase oxidation resistance of TiAl alloys at elevated temperatures by retarding oxygen diffusion into the alloys through the formation of Ti<sub>3</sub>Sn protective layer. It also promotes spallation resistance by creating Al<sub>2</sub>O<sub>3</sub> oxide pegs [64]. Pan et al. [64], analysed the impact of Sn addition on the oxidation performance of TiAl alloys with high Nb content. The alloy containing 3 at.% Sn displays superior oxidation resistance with the lowest mass gain of 3.29 mg/cm<sup>2</sup>, the thinnest oxide scale of 14  $\mu$ m and no spallation was observed. This is principally credited to the formation of the Ti<sub>3</sub>Sn phase which led to the formation of Al<sub>2</sub>O<sub>3</sub> oxide pegs. Also, the produced Al<sub>2</sub>O<sub>3</sub> oxide pegs offer mechanical locking between the oxide scale and substrate, therefore improving the spallation resistance. It is recognized that the oxidation of  $\gamma$ -TiAl alloy is always accompanied by spallation of oxide scales. This is because the scales of TiO<sub>2</sub> and Al<sub>2</sub>O<sub>3</sub> are loose and unable to act as an oxygen barrier for oxidation protection [64]. Hence, Sn addition enhances resistance to spalling of oxide scales.

Mn and Cr are characteristic  $\beta$ -stabilizers that could increase TiAl-based alloys RT ductility [16]. As an extraordinarily strong  $\beta$ -stabilizer, Singh et al. [106] examined the effects of Cr additions in Ti–45Al–8Nb alloy to produce diverse quantities of  $\beta$ -phase microstructure in as-cast TiAl alloys. It was observed that a rise in Cr content from 0 to 6 at.% led to the increase in volume fraction of the  $\beta$ -phase from 0.4% to 23% in the alloy. Also, the  $\beta$ -phase morphology changes to a highly “percolating” structure from a disperse fine particle-like appearance. This change in morphology contributed noticeably to the improvement recorded in the high Nb-containing  $\gamma$ -TiAl alloy hot-workability. But this alloy displayed poor creep and strength at elevated temperatures. Although bearing in mind the volume fraction of the  $\beta$ -phase which influences the creep

properties and strength at high-temperature, the  $\sim 8$  vol%  $\beta$ -phase equivalent to 2 at.% Cr addition was a very encouraging composition.

In a multi-alloying system examined by Panin et al. [95], the  $\beta$ -solidifying TiAl-alloy which is a new Russian alloy (Ti-44.5 Al-2 V-1 Nb-2 Cr/1 Zr-(0–0.1) Gd) were investigated. It was determined that the phase composition of the TiAl alloy in the as-cast state (without Gd) was characterized by three principal phases:  $\alpha_2$ ,  $\beta$  and  $\gamma$ . Alloys with Zr had a  $\beta$ -phase volume fraction that does not exceed 2–3%; while alloys with Cr showed  $\beta$ -phase volume fraction reaching 5–6% that was restricted along the transformed grains boundaries. It was discovered that the Zr-containing alloys showed grain boundaries lamellar colonies ( $\gamma+\alpha_2$ ) sprouts.

As stated earlier, the  $\beta$ -solidifying TiAl-based alloys properties are extremely dependent on compositions, particularly the  $\beta$ -stabilizing elements in the alloy. The mechanical properties and high-temperature deformability of a new TiAl alloy containing Nb and Mn were studied by Wu et al. [107]. It was deduced that the alloy had good hot deformability based on recorded low activation energy (392 kJ/mol) and low deformation resistance of the alloy. The primary lamellae were transformed completely into fine equiaxial  $\gamma$ -grains when compressed at the optimal deformation conditions 1200 °C/0.01 s<sup>-1</sup>. The billet microstructure composed largely of recrystallized  $\gamma$ -grains with high angle boundaries. It was reported that the alloy had UTS and elongation were 780 MPa and 1.44%, respectively, which benefits from the average size (4.9  $\mu\text{m}$ ) of the fine  $\gamma$ -grains.

Iron (Fe) is also known to be an effective  $\beta$ -phase stabilizer and could improve the liquidity of TiAl-based alloys. Fe leads to reduced lattice tetragonality of TiAl alloys because the atomic radius of Fe is smaller (1.27 nm) than Al (1.43 nm) [60]. It is known that  $\gamma$  and B2 phases increases as  $\alpha_2$ -phase reduces in TiAl-based alloys when Fe increases from 0 to 1.1 [60]. Consequently, Yang et al. [60] investigated the addition of Fe (0–1.1 at.%) in Ti43Al5Nb0.1B alloy produced by arc melting technique. It was reported that increasing the Fe content caused a reduction in the lattice tetragonality ( $c/a$ ) and average columnar grain width of the  $\gamma$ -phase. Fe led to B2-phase formation that is Fe-riched for both inter-dendritic and dendrite fields. It was reported that the compressive strain and strength were 1958.4 MPa and 29.8%, respectively, for the TiAl-based alloy at Fe 0.7 at.%. When Fe content is increased above 0.7 at.%, the mechanical properties depreciated because of B2-phase formation which typically behaves as crack initiation sites. It was also realized that Fe refines the grains and results in RT super-plasticity. The refinement of the microstructure was attributed to the Fe-rich band-like B2-phase that diminishes the rate of grain growth. While the formation of B2-phase was credited to the high-temperature  $\alpha$ -phase supersaturation that restrains the excess Nb and Fe. The Fe solid solution strengthening and grain refinement are responsible for the enhancement in the strain and strength.

## 2.2. Grain refinement

Owing to the dispersion strengthening effects of carbides, borides and silicides along with the formation of ternary compounds. C, B and Si are added to increases the physical, chemical, and mechanical properties of TiAl-based alloys. They also promote temperature characteristics like heat resistance, short-term and long-term strength components, durability, and hardness [108]. An element that has been of remarkable importance in TiAl-based alloys for grain refinement is boron (B) [12]. It was revealed by Imayev et al. [8], that thermally stable borides principally cause grain refinement effects and behave as heterogeneous nucleation sites during solidification and resultant phase transformations. This effectively promotes precipitation of homogeneous and fine microstructures in as-cast  $\gamma$ -TiAl-based alloys [12]. Grain refinement effects depend on the evolving order of phase transformation which is still an ongoing research topic. As an example, the effect of microalloying

on microstructure and phase stabilization could be understood by analysing the chemical composition of the borides. Oehring et al. [12], demonstrated that apart from borides, the rate of cooling also has a significant impact on the resultant microstructure and solid-state transformation of  $\beta/\alpha$  phase. During transformation, the morphology stems were said to be based on a solid-state reaction of  $\beta \rightarrow \beta+\alpha \rightarrow \alpha \rightarrow \alpha+\gamma \rightarrow \alpha_2+\gamma$ . It was concluded that refinement of microstructures causes the inhomogeneous distribution of  $\gamma+\alpha_2$  lamellae orientation followed by precipitation of  $\alpha$ -phase. It was deduced that  $\alpha$  nucleation at boride sites found in the inter-dendritic fields are larger in number than the orientations obtainable at the  $\alpha$ -phase. This nucleation occurs as borides precipitated from the  $\beta$ -phase at elevated temperature. Figure 2 shows SEM images in back-scattering electron (BSE) mode of as-cast and heat-treated TNM alloys, showing phase morphologies formed. For better understating of these phases, the reader is referred to ref [12].

In the work of Bazhenov et al. [104], Yttrium (Y) was added in the range of 0.02–0.6 at.% to a  $\beta$ -solidifying TiAl-based alloy and reported that Y promoted microstructural grain refinement. The presence of Y also contributed to increased strength and elongation. Due to its reactive element effects, Y also enhances heat resistance properties. It was concluded that 0.3 at.% addition of Y increases the hot-deformability of  $\beta$ -solidifying TiAl-based alloys. This is made possible because Y allows for the uniform oxide growth devoid of Ti and Al oxides layers. Imayev et al. [8], examined the effects of Al and the addition of additional microalloying elements in  $\gamma(\text{TiAl})+\alpha_2(\text{Ti}_3\text{Al})$  alloys produced by casting. It was shown that the microstructure was predominantly homogeneous and fine with no segregation when solidifying through the  $\beta$ -phase field at certain alloy compositions. This behaviour was ascribed to the effects of alloying transformation kinetics of  $\beta \rightarrow \alpha$  by avoiding the peritectic solidification path. Figure 3 indicates  $\beta$ -phase located at the layers of lamellae boundary colonies (Figure 3a) and significant coarsening of lamellae width shown in Figure 3b. Beta ( $\beta$ ) stabilizers like Mo, Nb, W and Cr do also contribute to refining microstructure grains by stabilizing the metastable B2-phase (ordered  $\beta$ -phase) at low temperatures, thereby, enhancing high-temperature deformability [9, 51]. Lately, the Ti-44Al-7Mo ternary alloy has drawn attention, with research works demonstrating that heat treatment procedure resulted in a considerable microstructural refinement with a substantial increase in hardness. In a review by Klein, Clemens, and Mayer [7], borides in TNM alloys was said to be off-stoichiometric caused by the alloying elements, thus, leading to vacancies or anti-site defects. The authors explained that Ti-borides in TiAl-based alloys barely display solubility for Al and consist basically of B and Ti. Hsu et al. [71], hypothesized that the effect of silicon (Si) is associated with grain refinement and dispersion hardening in TiAl alloy. It was noted that the quantity of primary  $\zeta$ -Ti<sub>5</sub>(Si, Al)<sub>3</sub> (silicide) precipitates increased as the content of Si increases leading to finer  $\alpha_2$  and  $\gamma$ -TiAl grains with decreasing volume fraction of lamellae. Addition of B has also been reported to be beneficial for both enhancements of strength and ductility especially in materials with duplex phase microstructures [11].

Titanium diboride (TiB<sub>2</sub>) has also been reported to refine TiAl-based alloys to a certain extent, but still retains the columnar crystal features. Han et al. [57], investigated the addition of 0.18–1.8 wt.% TiB<sub>2</sub> in cast 4822 alloy. It was realized that the characteristics of columnar structure does not change with the small addition of TiB<sub>2</sub> (0.18–0.36 wt.%) but promotes the reduction of the mean grain size to a certain degree. TiB<sub>2</sub> content of 0.54 wt.% in the as-cast microstructure produces an alloy which had columnar and equiaxed regions. However, a further increase in TiB<sub>2</sub> leads to complete equiaxed grains. This shows that TiB<sub>2</sub> addition has a threshold value for the refinement of TiAl alloy. It was further established that the fluidity of 4822 alloy could efficiently be enhanced by TiB<sub>2</sub> addition. It was concluded that 0.72 wt.% TiB<sub>2</sub> led to a reduction of the temperature range in the solid-liquid two-phase region and microstructural refinement resulted in fluidity enhancement.



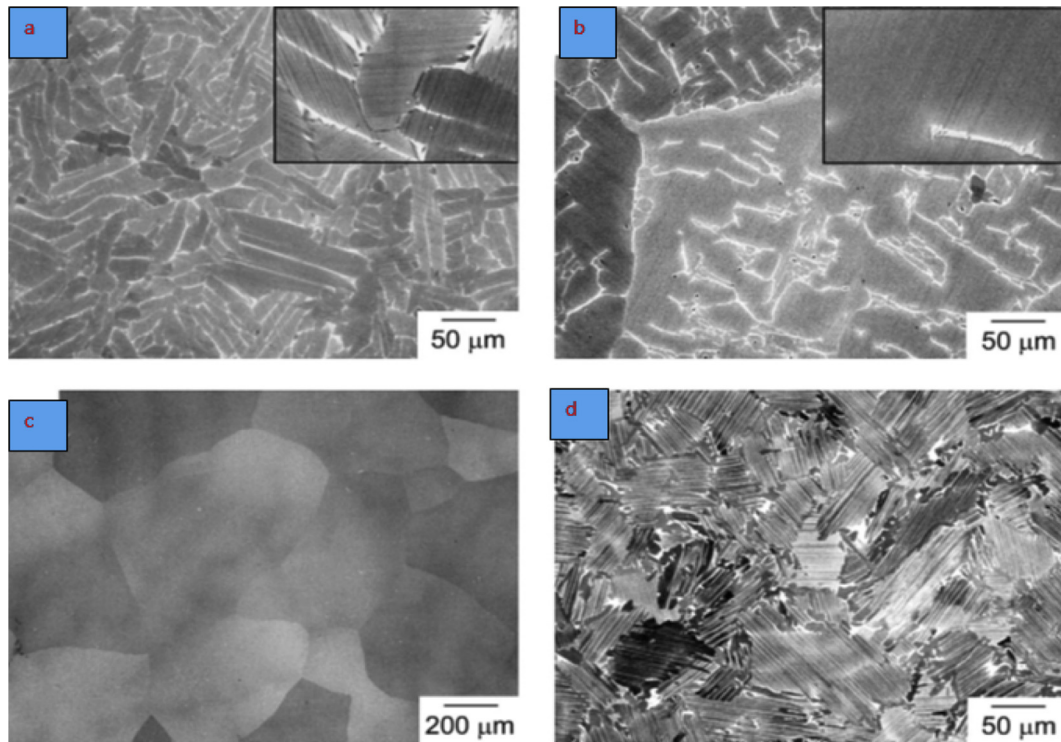


**Figure 2.** SEM Images of TNM alloy (a) As-cast (b) Heat-treated at 1310 °C/2 h/OQ/1450 °C/1 h/AC (c) Heat-treated at 1310 °C/2 h/OQ (d) Heat-treated at 1310 °C/2 h/OQ/1450 °C/1 h/FC as reported by ref [88].

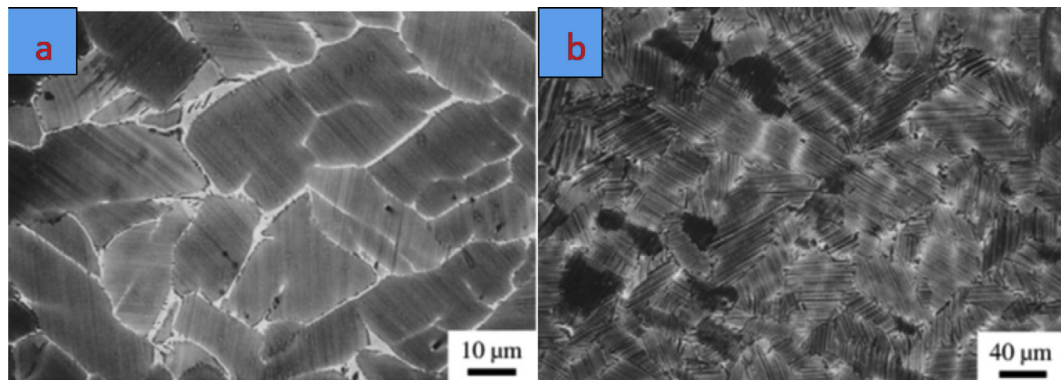


**Figure 3.** SEM Micrographs of TNM alloy (a) As-cast alloy (b) Heat Treated at 1450 °C/5 min/FC as reported by [8].

### 2.3. Formation of special phases ( $\omega_0$ -phase)

To achieve good oxidation resistance, creep, and high-temperature strength, Nb is usually added as alloying elements in TiAl-based alloys [15, 25, 99]. However, this causes increased hardness and leads to the formation of  $\omega_0$ -phase as an additional phase [19, 24, 99]. Typically, this  $\omega_0$ -phase precipitates in the  $\beta$ -matrix of  $\beta$ -solidifying TiAl-based alloys, but not the same for alloys where  $\alpha_2$ -phase precipitates [23, 25, 40, 99]. It is understood that the B2-phase is a thermodynamically metastable phase susceptible to decompose into  $\omega$ -related phases of trigonal- $\omega$ , D88- $\omega$  and B82- $\omega$  ( $\omega_0$ ) [25, 61]. The size and volume fraction of  $\omega_0$ -phase is strongly influenced by heat treatment and alloying elements, and also related to the  $\beta$ -stabilizing elements' diffusion [61, 109]. According to Yang et al. [61], during long time annealing,  $\omega_0$ -phase could be transformed to D88- $\omega$ -phase even though during WQ, the formation of  $\omega''$ -phase is unavoidable. Hence, the observation of B2/ $\gamma$  transition with adjacent  $\gamma$  lamellar discontinuous coarsening by the  $\gamma$ -phase nucleation in the

matrix of B2-phase. Also, structures containing  $\gamma$  and  $\omega$ -related phases are normally found in the B2 region.

Transmission electron microscopy (TEM) and other high-resolution microstructural examination equipment are adopted by different researchers in investigating the distribution of  $\omega_0$ . The  $\beta_0$ -phases are studied during the precipitation process that results in destabilization and stabilization of TiAl-based alloys. It was confirmed by Song et al. [25], that ordered  $\omega$  variants were observed to precipitate homogeneously inside the  $\beta_0$ -phase field of as-cast Ti-45Al-8.5Nb-0.2B alloy. In another study by Song et al. [97], as-cast Ti-45Al-8.5Nb-0.2W-0.2B-0.02Y alloy annealed at 900 °C and 950 °C exhibiting particles of micron-level  $\omega_0$ -phase precipitate in  $\beta_0$ -phases were investigated. It was discovered that the direct transformation of  $\beta_0(\omega_0) \rightarrow \gamma$  occurrence was only confirmed by TEM analysis. Also, the  $\omega_0$ -phase is Nb-rich with low W content in comparison to  $\beta_0$ -phase with almost the same composition of  $\beta_0$  and  $\gamma$  phases [97]. In alloys containing both  $\beta$  and  $\gamma$  stabilizers, there is no single  $\alpha$ -phase field in the



transformation sequence, instead there exist an  $\alpha+\beta+\gamma$  three-phase regime [23]. Likewise, Schloffer et al. [24], analyzed the cause of precipitation reactions during annealing after heating a TNM alloy above the  $\omega_0$ -solvus temperature. Figure 4a displays the histogram of Ti, Al, Nb and Mo as major alloying elements based on calculations made by Klein, Clemens, and Mayer [7] to quantify the chemical compositions. The authors also presented an atom probe tomography (APT) image reconstruction of Nb and Mo elements indicated in green and red lines, respectively, as shown in Figure 4b. The iso-concentration surfaces showed phases present and the elements inhomogeneous distribution. The concentration gradient adopted by Klein, Clemens and Mayer [7] was used in creating the surface with the  $\omega_0$ -particles. This demonstrated an elongated parallel arrangement along the direction of growth based on the orientation relationship [76]. From Figure 4, it could be deduced that the Ti, Nb and Mo atoms are not homogeneous, but the Al atoms are very close to being homogeneous. Also, it was realized that  $\omega_0$ -particles grow because of the redistribution of Mo that significantly affects the actual decomposition of phases. Other authors [2, 24, 97] have also concluded that there was Mo rejection from the  $\omega_0$ -phase, thereby, enriching the  $\beta$ -phase matrix.

The occurrence of  $\omega_0$  (ordered  $\omega$ ) phase at intermediate temperatures in TiAl-based alloys is widely reported [40, 61, 109]. Song et al. [109], studied the phase transformation behaviour of  $\omega_0$ -phase at 750–900 °C. It was realized that the microstructures comprise of  $\gamma+\omega_0$  with minor precipitates of  $\alpha_2$ -phase after ageing treatment followed by quenching from high temperature. A unique mechanism of twinning by the  $\alpha_2$ -phase was observed after ageing that seems analogous to the described mechanism of phase transformation diffusive-displacive in deformed TiAl alloys [40, 109]. This could provide a preferred site for  $\omega_0$ -phase initiation due to the twinned interface atomic structure being relative to the crystallographic arrangement of  $\omega_0$ -phase. Owing to the  $\gamma$ -phase precipitates from the stacking faults of  $\alpha_2$ -laths, a semi-coherent interface between  $\gamma$  and  $\omega_0$  phases are observed and high density of stacking faults is noticed inside the  $\alpha_2$ -laths. But the  $\gamma$ -phase direct nucleation from the matrix of  $\omega_0/\beta_0$  keenly develops at higher temperatures. The  $\omega_0$ -phase nucleates heterogeneously inside the  $\alpha_2$ -phase.

Apart from the  $\beta_0$ -phase, it is known that  $\omega_0$ -phase can be precipitated within the lamellar colonies after prolonged annealing by transformations of  $\alpha_2/\omega_0$  or  $\beta_0/\omega_0$  phases. Thus, it is essential for mechanical properties and microstructural stability. Besides the influence of V, Zr and Ta on microstructures, Song et al. [109] also investigated their influence on  $\omega_0$ -phase

stability. It was noticed that very fine-grained microstructure was obtained because of the multiple variants of  $\omega_0$ ,  $\gamma$  and  $\alpha_2$  phases formed from  $\beta_0$ -matrix at different orientation relationships. The overall orientation relationship based on interfaces formed is stated as:  $\{1120\}\omega_0//\{0001\}\alpha_2//\{111\}\gamma$ ;  $\langle 0001 \rangle\omega_0//\langle 1120 \rangle\alpha_2//\langle 101 \rangle\gamma$  [109]. The elements V, Zr and Ta were reported to harm the stability of  $\omega_0$ -phase, but the Ta appeared weaker than V and Zr.

#### 2.4. Strength improvement

The addition of C as an alloying element for TiAl-based alloys' high-temperature strength improvement has been widely studied. Moreover, C additions are usually employed for fatigue and creep resistance enhancement in TiAl-based alloys. Carbon controls the microstructure of FL ( $\alpha_2+\gamma$ ) through the refinement of the lamellar spacing owing to dislocation interactions between the fine lamellae [6]. Carbide precipitations and solution strengthening are the two methods of carbon strengthen alloys since it is an interstitial atom [4, 20, 54]. For TiAl-based alloys, C is located at the  $Ti_6$  octahedral cavities within Ti-atoms. In TiAl-based alloys for engineering applications, only the  $\alpha_2$ -phase possesses the  $Ti_6$  octahedral cavity that can accommodate C. This is due to its intrinsic solubility in  $\alpha_2$ -phase which is not obtainable in both  $\beta_0$  and  $\gamma$  phases. Also, segregation of C at the  $\alpha_2/\gamma$  interface deters  $\gamma$ -laths thickening thereby resulting in finer  $\gamma$  lamellae. Moreover, lath thickening reduction and increase in nucleation sites are major reasons for lamellar microstructure refinement in C-containing TiAl-based alloys [34]. However, Liu et al. [89] noticed that Nb addition contributed greatly to the rise in solid solubility of C in TiAl-based alloy reaching 2–3 at.% C. A requirement for C maximum solubility is obtained in the case of  $\gamma$ -phase relative to Al concentration which increases C solubility for Al-lean stoichiometric compositions [7]. This is corroborated by the excess Ti atoms occupying Al sites and creating  $Ti_6$  octahedral cavities to accommodate C. Addition of transition metals as an alloying element enhances the solubility within the  $\gamma$ -phase for interstitial elements [4, 54, 89]. This is because they prefer to occupy the  $L1_0$  lattice of Ti sites. Nevertheless, the stoichiometric B2 structure has no site that can encourage the  $\beta_0$ -phase by substituting atoms of transition metals, thus, limiting solubility of interstitial atoms like C [7]. Schwaighofer et al. [110], studied the addition of 0.75 at.% C in a TNM alloy using APT to determine the phase compositions present which agreed with Klein, Clemens, and Mayer [7]. The latter explained that the incorporation of C increases

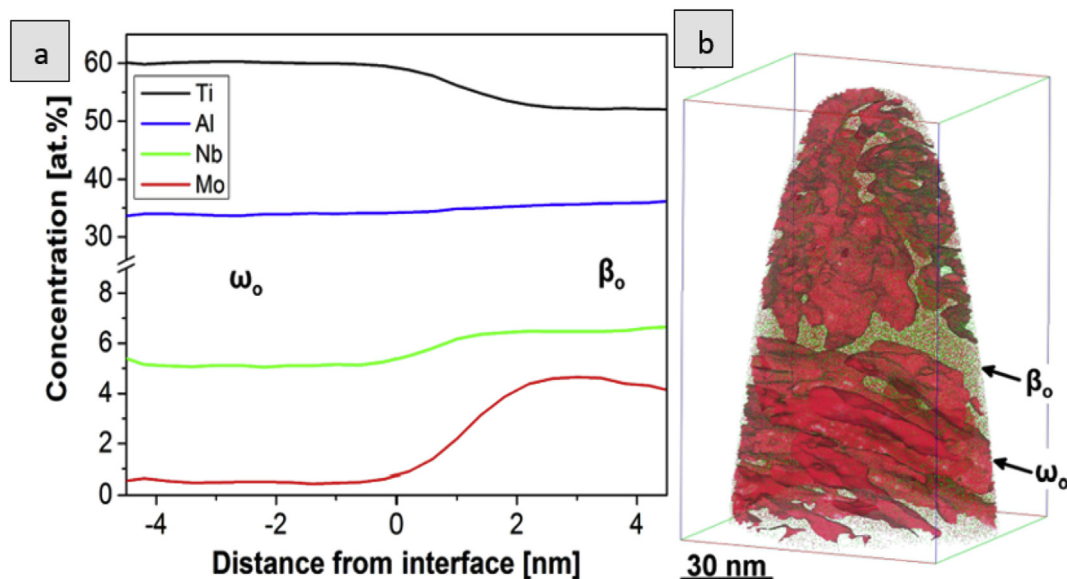


**Figure 4.** Showing the (a) proximity histograms across the interfaces (b) APT reconstruction containing  $\beta_0$  and  $\omega_0$  phase Nb (green) and Mo atoms (red) were indicated as reported by [7].

nano-hardness by solution strengthening to form carbides within the  $\alpha_2$  and  $\gamma$  phases verified by APT. However, owing to poor solubility of C in the  $\beta_0$ -phase, an increase in the overall C content diminishes the nano-hardness of the  $\beta_0$ -phase. Hence, C is said to be an  $\alpha_2$ -phase stabilizer [3].

In the work of Li et al. [6], the influence of C on the elevated temperature mechanical properties of Ti-43Al-6Nb-1Mo-1Cr alloys was investigated. It was reported that 0.5 at.% C increases both the elongation and UTS of the alloy as: 7.07% and 643.85 MPa (at 800 °C), 23.55% and 540.02 MPa (at 850 °C) with 40.5% and 389.82 MPa (at 900 °C), respectively. At elevated temperatures, a reduction in elongation is observed for C content between 0.5 to 1.0 at.%; while the UTS increases. This is ascribed to the decreasing lamellar ( $\alpha_2+\gamma$ ) colonies sizes, equiaxed crystals transformation to columnar crystals, the disappearance of segregations and carbides developments. Since C is an  $\alpha/\alpha_2$  stabilizer, it causes the eutectoid temperature to increase and shifts solidification path in TNM alloys to L/L+ $\beta$ /L+ $\alpha$ + $\beta$ / $\alpha$ + $\beta$  from L/L+ $\beta$ / $\beta$ / $\alpha$ + $\beta$  [6].

Furthermore, Liu et al. [89] reported that C addition of 5 at.% changes the solidification pathway of Ti-46.6Al-7.5Nb-0.5Si-0.2B to L  $\rightarrow$  L + H(Ti<sub>2</sub>AlC)  $\rightarrow$  L+ $\alpha$ +H  $\rightarrow$   $\alpha$ + $\gamma$ +H  $\rightarrow$   $\gamma$ + $\alpha_2$ +H from L  $\rightarrow$  L+ $\beta$   $\rightarrow$   $\beta$ + $\alpha$   $\rightarrow$   $\alpha$   $\rightarrow$   $\alpha$ + $\gamma$   $\rightarrow$   $\gamma$ + $\alpha_2$ . The as-cast microstructure was reported to comprise of FL ( $\alpha_2+\gamma$ ) microstructure and eutectic silicide at the dendritic region. A large quantity of randomly dispersed primary Ti<sub>2</sub>AlC particles was detected in the dendritic region. The Ti<sub>2</sub>AlC primary carbide gave microhardness value of about 1068 HV leading to the increment from 325 to 917 HV of the matrix. Song et al. [111], investigated the effects of C on Ti-46Al-8Nb-0.7C alloy at intermediate temperatures. Equiaxed  $\gamma$ -grains at lamellar boundaries with decomposed  $\alpha_2$ -laths were noticed at higher stress and creep temperatures. The induced H-carbide precipitation at the interface of  $\gamma/\alpha_2$  lamellar results in the transformation of the  $\alpha_2$ -laths. The high-temperature stabilization of P-carbides in the  $\gamma$ -grain interior reduces at high creep temperatures which barely affected the P-carbides precipitation and morphology development.

The influence of C addition on a dual-phase Ti-46Al-4Nb alloy with respect to hardness and microstructure was investigated by Cabibbo [34]. It was demonstrated that an increase in hardness leads to diminishing lateral size in the twinning of  $\gamma$ -phase invariably obstructing sliding of the dislocations. It was shown that hardness of TiAl alloy was largely dependent on  $\alpha_2$ -phase volume fraction and quantity of C it dissolves. Bazhenov et al. [104], studied the effect of 0.8 at.% Zr+0.2 at.% Y and 2.3 at.% Y on mechanical properties of TNM-B1 alloys. The microstructural analysis revealed that  $\alpha_2$ ,  $\gamma$ , and  $\beta$  phases were low in Y content and Al<sub>2</sub>Y contained virtually all the Y. The addition of Y reduces tensile strength and elongation property of the TNM-B1 alloy. Large Al<sub>2</sub>Y-phase was observed after 2.3 at.% Y addition at the colonies  $\alpha_2+\gamma$  boundaries; while increased  $\beta$  quantity causes a reduction in mechanical properties. The UTS and El decrease due to Y addition of up to 2.3 at.% in the TNM-B1 alloy. Also, a slight reduction in mechanical properties was noticed with the combined addition of 0.2 at.% Y and 0.8 at.% Zr. The presence of massive quantities of Al<sub>2</sub>Y and  $\beta$  phases is responsible for the reduction in TNM-B1 alloy mechanical properties.

Furthermore,  $\beta_0$ -phase tends to be partitioned by Mo, thereby, reducing  $\beta_0$ -phase and increasing Mo in this phase which restrains  $\omega_0$ -phase formation. A reduction in the nano-hardness is effected through the privation of  $\omega_0$ -phase within  $\beta_0$ -phase of the C-containing TiAl alloy as there are no precipitation hardening occurring. Studies investigating the influence of C in TiAl-based alloys have mostly being about decreasing the recrystallization kinetics and stabilization of the microstructure [112]. Klein, Clemens, and Mayer [7], also reported that C increases the stability of TNM alloys microstructure. This is due to solute-drag effects and strong partition of C by weak redistribution restraining recrystallization of new grains being formation. Precipitation initiates immediately the  $\alpha_2$ -phase is saturated within the interstitial elements.

### 3. Characteristic effects of silicon additions in TiAl alloys

Si-containing TiAl alloys are potential materials for elevated temperature utilization in the aerospace and automobile industries. Addition of Si to TiAl-based alloys as an alloying element is often controversial. Discussions available in literature are usually on microstructural stability and creep resistant associated with Si addition [4, 54, 112, 113]. However, Si is known to be a highly promising alloying element in improving elevated temperature strength of Ti-Al alloy systems [38, 114]. This is due to the Ti<sub>5</sub>Si<sub>3</sub>-phase ( $\zeta$ -silicide; HCP structure) formed that acts as a strengthening phase for composites' reinforcement based on TiAl intermetallic alloys [115]. Silicide ( $\zeta$ -Ti<sub>5</sub>Si<sub>3</sub>) is an intermediate phase that has considerable stiffness with superb oxidation and corrosion resistance [38]. Thus, Si is well suited for enhancing oxidation resistance through the formation of Ti<sub>5</sub>Si<sub>3</sub>-phase. Ti-Al based alloying systems with Si are identified at the  $\alpha_2/\gamma$  lamellar interfaces with precipitates of  $\zeta$ -silicide (Ti<sub>5</sub>Si<sub>3</sub>) known to be responsible for diminishing the dislocation mobility and interfacial stability [7, 54, 116, 117]. Si addition of  $\sim$ 0.5 at.% results in the formation of fine Ti<sub>5</sub>Si<sub>3</sub> particles; while between 2.0-6.0 at.% of Si produces large Ti<sub>5</sub>Si<sub>3</sub> particles or whiskers nucleated at  $\gamma/\gamma$  and  $\gamma/\alpha_2$  interfacial sites [3, 113]. This tends to align particles at the interface of lamellae, particularly for alloys that have low quantity of  $\alpha_2$ -phase after heat treatments in the dual-phase region. The Ti<sub>5</sub>Si<sub>3</sub> precipitate formation is desirable for resistance to creep through phase stability improvements and dislocation motion prevention [116]. The precipitation of Ti<sub>5</sub>Si<sub>3</sub> from Si-bearing TiAl alloys in the  $\gamma$ -phase occurs heterogeneously and the nucleation depends on the dislocation types [113]. Owing to poor Si solubility in the  $\gamma$ -phase, precipitation of silicide emerges when the  $\alpha_2$ -phase which dissolves most of the Si is reduced in quantity. According to Sun and Froes [113], a true-twin type  $\gamma/\gamma_T^*$  lamellar boundary is a Ti<sub>5</sub>Si<sub>3</sub> precipitate-free  $\gamma/\gamma$  boundary because of its low boundary energy. Also, the growth of needle-like Ti<sub>5</sub>Si<sub>3</sub> particles at the  $\gamma/\gamma$  boundaries is regulated through interfacial diffusion of Si. Moreover, the growth of rounded Ti<sub>5</sub>Si<sub>3</sub> particles in the  $\gamma$ -matrix is controlled by the volume diffusion of Si, where the Ti<sub>5</sub>Si<sub>3</sub>/ $\gamma$  interfaces are incoherent.

It has been reported by Du, Wang and Zhu [116], that Si added to cast TiAl-based alloys are found to be beneficial to creep resistance enhancement without sacrificing the tensile properties. Si of 0.3 at.% in Ti-47Al-2Cr-1Nb-0.8Ta-0.2W-0.15B-0.3Si alloy produced through powder metallurgy (PM) resulted in unfavourable resistant to creep effects. It was concluded that the creep mechanism was not affected by Si addition, but influences the microstructural stability. Si was reported to be situated at the lamellar interfaces with precipitates of silicide and recrystallized  $\gamma$ -phase. Generally, Si atoms are located inside the matrix as solute due to the powder metallurgy process. Thus, making the detrimental effects more serious than the benefits of Ti<sub>5</sub>Si<sub>3</sub> precipitates given rise to poor creep resistance of the alloy. Also, Karthikeyan and Mills [112] assert that Si and C have considerable influence at all creep stages in diminishing the strain rates through precipitation hardening. Microstructural stability before creep, increases creep resistance through the elimination of metastable  $\alpha_2$ , precipitates nucleation and lowering dynamic recrystallization driving force in alloys containing Si and C. Silicon was also reported to improve oxidation resistance, but also reduce the oxidation resistance when Si quantity is increased. However, Jiang et al. [72] reported that Si and Nb combinations could be beneficial to improve TiAl alloy resistant to oxidation substantially.

TNM alloys usually have a high amount and varying quantity of  $\alpha_2$  and  $\beta_0$  phases, respectively. A two-step heat treatment is suggested because these phases change the reaction sequences in TNM alloys due to Si addition producing nano-lamellar structures [3, 4]. This makes the  $\gamma$ -phase lamellar to be formed inside the grains of  $\alpha_2$  by adequate thermal activation owing to the alterations in crystal structure created by two Shockley partial dislocations [7]. Klein et al. [1], heat-treated Ti-43.5Al-4Nb-1Mo-0.1B-0.3C-0.3Si alloy for 15 min at 1350 °C with oil quenching. This was followed by annealing at 800 °C between 15 min

to 24 h and furnace cooled. The microstructural image is shown in Figure 5. The SEM image could not resolve the ultra-fine structure of the lamellar colonies of  $\alpha_2/\gamma$ -phases. This was made known by the transmission emission microscopy (TEM) as observed in Figures 5a and 5b. However, only the prior  $\beta_0$ -phase that decomposed into  $\gamma$ -platelets and  $\omega_0$ -particles with few undissolved  $\beta_0$ -phases during annealing could be resolved by SEM. The  $\gamma$ -lamellar formed from the transformation of  $\alpha_2$ -grains tend to align parallel through the mechanism known as the BOR [37]; that has been explained by several authors [51, 76, 81]. Also, it was observed by Klein et al. [1], that the  $\zeta$ -Ti<sub>5</sub>Si<sub>3</sub> precipitates were not noticed around the lamellar interface.

In a study conducted by Lee et al. [114], ternary Ti–Al–Si alloy was synthesized through mechanical milling followed by SPS to examine their plastic deformation behaviour. The microstructure was rich in thermodynamically stable phases of  $\alpha_2$ -TiAl<sub>3</sub> and  $\zeta$ -Ti<sub>5</sub>Si<sub>3</sub> intermetallics formed through invariant reaction. The initial powder structural properties and plane defects of sintered product influenced the brittle-ductile transition, thereby, increasing the fracture toughness of the Ti<sub>5</sub>Si<sub>3</sub> alloy. The Crystallographic patterns and microstructure exposed the stacking faults or twinning brought about by the acute plastic deformation. This is attributed to the phases of Ti<sub>5</sub>Si<sub>3</sub>(HCP) or TiAl<sub>3</sub>(FCC) slip system which is dependent on the refined grains and intermetallics nucleated at ambient temperature. Based on the crystallographic nature of metallic materials, BCC and FCC demonstrate satisfactory slip system while HCP displays inadequate slip system with temperature-dependence.

Knaislova et al. [38], studied the oxidation behaviour of Ti–Al–Si alloys prepared by PM at elevated-temperature. The alloy (TiAl10Si30) having the highest content of silicon gave the best resistance to oxidation through repetitive heating and cooling. The chemical reaction of the alloy displays good adhesion with the oxide layer and diffusion growth which is influenced by the high Si content. The Ti–Al–Si alloy had high microhardness after annealing at 1000 °C for 400 h. The hardness values remain the same even with prolonged oxidation time. In a related study by Knaislova et al. [115], phase composition, microstructure and hardness of Ti–Al–Si alloy fabricated through MA + SPS were examined. After compaction, the alloy (TiAl15Si15) contained uniform microstructure of small quantity of TiAl<sub>2</sub> and Ti<sub>5</sub>Si<sub>3</sub> in TiAl-matrix. Due to fine Ti<sub>5</sub>Si<sub>3</sub>-phase, the alloy microhardness rises to 865 ± 42 HV<sub>5</sub>. Apart from the TiAl<sub>2</sub>-phase, the phase composition observed was the same as in Knaislova et al. [38], independent of preparation conditions. It was also reported that the porosity is exceptionally low but has better hardness, UTS, and abrasive wear resistance compared to the similar alloy in ref [38] produced through SPS combined with reactive sintering.

In another work by Knaislova et al. [117], mechanical properties, phase compositions and microstructure of ternary Ti–Al–Si alloys produced by arc melting were investigated. The findings were compared with Ti–Al–Si produced by MA + SPS. The arc melted alloy is had a structure of very coarse Ti<sub>5</sub>Si<sub>3</sub> in TiAl-matrix with porosity and cracks. Fast cooling of the melting metallurgy was suggested to be responsible for the cracks observed in the alloy. The PM processed alloy had a regular structure of fine-grains, low porosity, and high value of microhardness. Microhardness value record for samples processed by MA + SPS was almost twice the values recorded by the arc-melted Ti–Al–Si alloys. It was concluded that the melting process needs to be optimized to reduce the material porosity.

It has been reported by various authors [1, 3, 51] that Si dissolves by substituting for Al as determined by ab initio calculations. This leads to Al deficiencies in Si-containing TiAl-based alloys, but strong  $\beta$ -stabilizers like Mo if present would substitute for Ti which relocates to the Al-sites. While the Ti is diminished for the off-stoichiometry  $\alpha_2$ -phases with increasing Al content. Interstitial elements like C and Si with substitutional elements such as Mo, Nb and Cr would tend to balance the TiAl-based alloy chemistry to provide an equilibrium between high-temperature creep resistance and ductility [54]. The crystal structure of the  $\alpha_2$ -phase with the energetical chemical environment makes Si preferentially substitute Al [3, 4]. Typical TNM alloys are composed of a significant amount of  $\alpha_2$ -phases far more than  $\gamma$ -TiAl with Al content between 45–48 at.%. The  $\alpha_2$ -phase of the TNM alloys stores almost all quantities of Si present; thereby, determining the overall solubility and/or precipitation of Si. Thus, limited or no interfacial precipitation occurs because of almost complete dissolution of Si within the  $\alpha_2/\gamma$  colonies. However, the ordered structure of  $\alpha_2$ -Ti<sub>3</sub>Al and  $\gamma$ -TiAl made TiAl-based alloys brittle but studies have shown that elements like Nb, Mo, Mn, V and Cr could alter the volume of the unit cell, modify the density distribution of electrons and re-order bonding. Thus, producing TiAl alloys with better ductility and fracture toughness.

#### 4. Applications and future outlook

This section succinctly enumerates the various fields of application where TiAl-based alloys are being employed and give an impetus for future works on these types of intermetallic alloys.

##### 4.1. Typical application of TiAl-Based alloys

It is common knowledge that there is no ‘one cap fits all’ composition of alloys meant to serve for all purposes. However, alloy compositions are

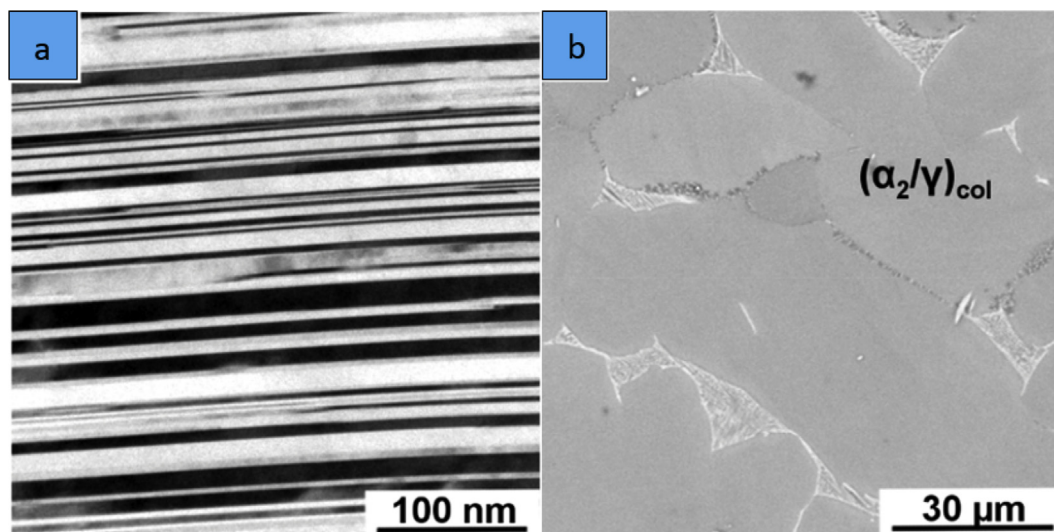


Figure 5. (a) TEM Image and (b) SEM Micrograph of two-step heat treated TNM alloy by Klein et al. [1] and reported by Klein, Clemens and Mayer [7].



typically adapted in combination with the appropriate production techniques to accomplish desired properties for a specific use. Currently, Ti alloys account for one-third of modern aircraft engines' weight after nickel-base superalloys; which is the second commonly used material [103]. Although processing Ti alloys are expensive which hamper its economic viability, the aerospace industry is a multi-billion-dollar industry where performance and safety are paramount [83].

In the manufacturing of critical components subjected to corrosive environments and high-temperatures, TiAl is a potential alternative material employed in the field of automobile and aerospace [77]. Weight saving is of prime concern for flight and TiAl alloys have an excellent strength-to-weight ratio in comparison to aluminium, nickel, and steel alloys. This is expected to allow producers of the aircraft to decrease the overall weight, thereby, minimizing fuel consumption and expenses [14, 83]. In 2006 General Electric (GE) introduced Ti-48Al-2Cr-2Nb alloy to fabricate LPT blades of their GENx engines used by aeroplanes of Boeing's 747-8s and 787s [109, 111]. The PW1100G Geared-TurboFan (GTF) engines' LPT blades was developed using a TNM alloy. Also, the same TNM alloy was used for LEAP™ engine LPT blades by SNECMA [14]. In comparison to other class of engines, GENx engines deliver 50% noise reduction, 20% increment in fuel efficiency, and 80% NOx emission reduction [30, 83]. Although, feasibility studies for the TiAl-based alloy high-pressure compressor have been conducted by Snecma and Turbomeca. The GE 4822 alloy LPT blade is still the most commercially available intermetallic component in service. Pratt & Whitney including Volvo has also been conducting thorough work on TiAl-based alloys to develop parts like turbine dampers, blade retainers, shrouds, and compressor blades [14, 30]. The potential of TiAl-based alloys for turbine engines is well recognized by major manufacturers in the aerospace industry. However, aerospace engineers are faced with the obstacle of overcoming poor oxidation resistance at an elevated temperature when designing aircraft's engine components [83].

The automotive industry has also seen increased applications of TiAl-based alloys. Some parts are now being fabricated using TiAl alloys owing to high-temperature resistance, low density, and high fatigue strength [83]. It is used for piston connecting rods of sports cars because it reduces vibration in the damping system. Also, due to high-temperature strength and low density, it is used for engine valves allowing the formation of lasting, but valves with lightweight that could improve engine operations. Owing to weight reduction, it has found usage in making valve cups. Mitsubishi Motors was reported to have used TiAl alloy in their diesel or gasoline engines of Lancer 6 model as turbine wheels of turbochargers in high-performance racing cars [14].

They have found extensive use in gas turbines due to their attractive mechanical properties [118]. Nevertheless, TiAl poor resistant to oxidation above 800 °C is still inadequate. TiAl-based alloys are reported to be extensively utilized for corrosion prevention in seawater environments and ideal in chemical and petrochemical industries; due to their chemical and mechanical properties [83]. TiAl-based alloys remain one of the highly biocompatible materials. Hence, it is used in biomedical applications as implants for orthopaedic, dental, and cardiovascular applications. This is because of its non-immunogenic, non-toxic, and high strength-to-density ratio in addition to its remarkable corrosion resistance property [119].

The past two decades have seen intense industrial collaborations to advance and produce novel materials based on TiAl alloys. For instance, Pratt & Whitney and General Electric (GE) are highly involved in different collaborations. This is done to develop an innovative TiAl-based alloy that could operate at higher temperatures for applications in advanced aircraft turbo engines. Specifically, Pratt & Whitney had a Cooperative Research and Development Agreement (CRADA) with Lawrence Livermore National Laboratory to produce TiAl-based alloy materials of improved ductility and toughness for commercial jet engines

[120]. Collaborations are however not limited to industries. Some other research groups are participating tremendously towards the advancement of novel TiAl-based alloys to further enhance the properties of previously established TiAl alloys [22, 81].

#### 4.2. Future outlooks, challenges and prospects

Intermetallic  $\gamma$ -TiAl-based alloys fulfil various crucial prerequisites for lightweight structural applications in the automotive and aerospace industries [9, 14, 22, 101]. As stated earlier, Ti-Al alloying systems are potential weight saving high-temperature materials. However, they are rather quite expensive to manufacture owing to their poor machinability, hot-workability and castability [10, 17, 30]. It should be noted that because of the inherent brittleness of TiAl, processing through the wrought techniques must be conducted at elevated temperatures (normally above 1100 °C) and multistep operations of low deformation rates [30]. This requires using distinct equipment in specific gas atmospheres. Solidification during melting metallurgy has often led to microalloying elements segregation and macroscopic columnar grains. This method has been presented to demonstrate greater microstructural flexibility. Also, it has the benefit of improved ductility through thermal-mechanical treatments, so that equiaxed or finer duplex microstructures could be attained [30]. Nevertheless, the manufacturing of these alloys is still problematic. Melting metallurgy is confronted with the issue of high reactivity of melt with melting crucibles, high melting points of intermetallic phases, exothermic reactions during intermetallic phase formation and cracks and pores formation [115]. All these difficulties associated with wrought processing motivated researchers to study additive manufacturing (AM) technology for producing TiAl-based alloy products [11, 14, 30, 31, 101, 121].

The application of different additive manufacturing (AM) technologies to fabricated TiAl-based alloys in the past two decades have gained considerable interests. The most widely used AM technology in processing composites is Selective Laser Sintering/Melting (SLS/M), Laser Engineered Net Shaping (LENS), Electron Beam Melting (EBM) and Fused Deposition Modelling (FDM) [120]. The benefit of AM is the direct production of complex shapes, near-net-shaped parts of high quality, uniform components with minor post-processing and a significant reduction in scraps [30]. Due to the high precision in AM techniques, it could be used to make several aerospace components with complex shapes from TiAl-based alloys. Among the AM technologies, LENS, EBM and SLS have been successfully used in the development of TiAl alloys [31, 43, 81, 101, 122, 123].

Even though these technologies display realistic capacity, most works are still been focussed on achieving fully dense parts with least defects through processing parameters optimization. Currently, EBM is found to display maximum readiness in term of technical feasibility [30]. Most AM suffers from high thermal gradient created by the high cooling rate and low substrate temperature leading to complex phase transformations due to high-energy input and thermal history [47]. Also, uneven distribution and evaporation of Al result in inhomogeneous mechanical properties of TiAl alloy fabricated by AM technologies. This gives rise to density variations and subsequently leads to reduced strength of final parts [120].

As reported earlier,  $\beta$ -stabilizing  $\gamma$ -TiAl-based alloys are gaining awareness because they display outstanding workability with large-scale production opportunities [124]. However,  $\beta$ -phase hardness is dependent on the type of  $\beta$ -stabilizing element in the TiAl alloys. Cr, Mn, and V have been reported to produce  $\beta$ -phase of low hardness while Nb, Mo and W promote  $\beta$ -phase with high hardness in TiAl alloys. Consequently, decreasing the  $\beta$ -phase hardness could prove to be helpful in the enhancement of  $\beta$ -solidifying TiAl-based alloys' ductility. Also, alloying elements' composition determines the resultant microstructures which directly influences the elevated temperature mechanical properties of

$\gamma$ -TiAl alloys. Thus, to improve its intrinsic ductility, it is essential to control the microstructural evolution. This could be achieved by adding alloying elements such as W, Mo, Nb, V, C and Mn which could also help in grain refinements or phase stability and further promote hot workability. This could be followed by a multi-stage heat treatment procedure and hot-pack or near-isothermal working. Previous works have shown that TiAl-based alloys' plastic deformation is primarily restricted to the  $\gamma$ -TiAl phase. This is due to the ordinary dislocation glides, but the deformation mechanism occurs by mechanical twinning. Consequently, the  $\gamma$ -phase refinement would help enhance TiAl-based alloys' mechanical properties [105]. Whereas, if the microalloying element diffusivity is lower than Ti,  $\alpha_2/\gamma$  phase boundary migration process could be hampered through discontinuous coarsening. Besides, the tendencies of alloying elements'  $\beta$ -stabilizing order of effects would be very beneficial in the designing of TiAl-based alloys' composition and microstructure to improve the mechanical properties; while mitigating the precipitation of the unwanted  $\omega$ -related phases.

Briefly, the basis for the effective application of TiAl-based alloys as structural engineering materials is determined by efficiently adjusting the microstructure. This is attained through proper alloying and carefully tailored processing. This should improve the mechanical properties, especially ductility when the alloying element can stabilize and promote new microstructures. Therefore, it is pertinent and essential to recognize the basics of processing, alloy designs, microstructural characterization, the relationship between property and microstructure, characteristics of new alloys together with the effects during service. Moreover, it has been demonstrated that AM could be combined with hot deformation techniques in achieving good workability and microstructural flexibility. It is expected that combination of a suitable AM technology such as EBM and LENS followed by multi-step heat treatment and hot working at intermediate temperatures would produce a unique combination of properties. This could be used for fabricating novel materials in the automotive and aviation industries. Finally, the increasing interests in structural engineering parts that could be used in automotive and aerospace applications are expected to consistently encourage more research in developing TiAl-based alloy components. Predictably, this same manner of inclination will continue for many more years to come.

## 5. Conclusions

1. The relatively newly developed  $\gamma$ -TiAl-based alloys are increasingly being applied into aero and automobile engines. Particularly, the  $\beta$ -solidifying TNM alloys having balanced mechanical properties and hot workability.
2. The beta phase ( $\beta$ -phase) is a detrimental phase at the materials' service temperatures which could be easily reduced and/or completely removed with appropriate heat treatment technique. This arises from the  $\beta$ -phase transformation to the hard and brittle  $\beta_0$ -phase that is incompatible with the  $\gamma$  and  $\alpha_2$  phases resulting in crack nucleation and propagation at the  $\beta_0/\gamma$  interfaces. Hence, a decrease in the ductility at the service temperature.
3. Nb and Mo (both  $\beta$ -stabilizers) are vital alloying elements providing improved creep resistance, oxidation resistance and elevated temperature strength retention.
4. Apart from grain refinements, boron is also beneficial for both enhancement of strength and ductility specifically for materials with duplex phase microstructures.
5. The  $\omega_0$ -phases precipitates within the  $\beta$ -matrix for  $\beta$ -solidifying  $\gamma$ -TiAl-based alloys but not the same for alloys where  $\alpha_2$ -phase precipitates. This  $\omega_0$ -phase are not easily resolved by SEM analysis except by TEM and other high-resolution microstructural analysis equipment.
6. The addition of Si to TiAl-based alloys influences creep resistance and stabilizes the microstructures but Si as an alloying element is rather controversial.

## Declarations

### Author contribution statement

All authors listed have significantly contributed to the development and the writing of this article.

### Funding statement

The authors would like to acknowledge the financial support of African Laser Centre-National Laser Centre; Council for Scientific and Industrial Research, South Africa (ALC-NLC; CSIR), Project Number LHIP500 Task ALC S100.

### Competing interest statement

The authors declare no conflict of interest.

### Additional information

No additional information is available for this paper.

## References

- [1] T. Klein, B. Rashkova, D. Holec, H. Clemens, S. Mayer, Silicon distribution and silicide precipitation during annealing in an advanced multi-phase  $\gamma$ -TiAl based alloy, *Acta Mater.* 110 (2016) 236–245.
- [2] J. San Juan, P. Simas, T. Schmoelzer, H. Clemens, S. Mayer, M.L. N3, Atomic relaxation processes in an intermetallic Ti–43Al–4Nb–1Mo–0.1 B alloy studied by mechanical spectroscopy, *Acta Mater.* 65 (2014) 338–350.
- [3] M. Kastenhuber, T. Klein, H. Clemens, S. Mayer, Tailoring microstructure, and chemical composition of advanced  $\gamma$ -TiAl based alloys for improved creep resistance, *Intermetallics* 97 (2018) 27–33.
- [4] M. Kastenhuber, B. Rashkova, H. Clemens, S. Mayer, Enhancement of creep properties and microstructural stability of intermetallic  $\beta$ -solidifying  $\gamma$ -TiAl based alloys, *Intermetallics* 63 (2015) 19–26.
- [5] M. Burtscher, T. Klein, S. Mayer, H. Clemens, F.D. Fischer, The creep behavior of a fully lamellar  $\gamma$ -TiAl based alloy, *Intermetallics* 114 (2019) 106611.
- [6] M. Li, S. Xiao, Y. Chen, L. Xu, J. Tian, The effect of carbon addition on the high-temperature properties of  $\beta$  solidification TiAl alloys, *J. Alloys Compd.* 775 (2019) 441–448.
- [7] T. Klein, H. Clemens, S. Mayer, Advancement of compositional and microstructural design of intermetallic  $\gamma$ -TiAl based alloys determined by atom probe tomography, *Materials* 9 (9) (2016) 755.
- [8] R.M. Imayev, V.M. Imayev, M. Oehring, F. Appel, Alloy design concepts for refined gamma titanium aluminide-based alloys, *Intermetallics* 15 (4) (2007) 451–460.
- [9] P. Erdelyi, P. Staron, A. Stark, T. Klein, H. Clemens, S. Mayer, In situ and atomic-scale investigations of the early stages of  $\gamma$  precipitate growth in a supersaturated intermetallic Ti–44Al–7Mo (at.%) solid solution, *Acta Mater.* 164 (2019) 110–121.
- [10] V.M. Imayev, A.A. Ganeev, T.I. Nazarova, R.M. Imayev, Effect of hot forging in the ordered phase field on microstructure and mechanical properties of  $\beta$ -solidifying  $\gamma$ -TiAl alloys, *Letters on Materials* 9 (4s) (2019) 528–533.
- [11] V. Singh, C. Mondal, R. Sarkar, P.P. Bhattacharjee, P. Ghosal, Compressive creep behavior of a  $\gamma$ -TiAl based Ti–45Al–8Nb–2Cr–0.2 B alloy: the role of  $\beta$  ( $\beta_2$ )-phase and concurrent phase transformations, *Mater. Sci. Eng., A* 774 (2020) 138891.
- [12] M. Oehring, A. Stark, J.D.H. Paul, T. Lippmann, F. Pyczak, Microstructural refinement of boron-containing  $\beta$ -solidifying  $\gamma$ -titanium aluminide alloys through heat treatments in the  $\beta$  phase field, *Intermetallics* 32 (2013) 12–20.
- [13] J. Tian, D. Zhang, Y. Chen, G. Zhang, J. Sun, Effect of nano Y2O3 addition on microstructure and room temperature tensile properties of Ti–48Al–2Cr–2Nb alloy, *Vacuum* 170 (2019) 108779.
- [14] P.V. Cobbinah, W.R. Matizamhuka, Solid-state processing route, mechanical behaviour, and oxidation resistance of TiAl alloys, *Advances in Materials Science and Engineering* 2019 (2019) 1–21.
- [15] O. Ostrovskaya, C. Badini, G. Baudana, E. Padovano, S. Biamino, Thermogravimetric investigation on oxidation kinetics of complex Ti–Al alloys, *Intermetallics* 93 (2018) 244–250.
- [16] N. Cui, Q. Wu, K. Bi, T. Xu, F. Kong, Effect of heat treatment on microstructures and mechanical properties of a novel  $\beta$ -solidifying TiAl alloy, *Materials* 12 (10) (2019) 1672.
- [17] G.H. Liu, T.R. Li, X.Q. Wang, R.Q. Guo, R.D.K. Misra, Z.D. Wang, G.D. Wang, Effect of alloying additions on work hardening, dynamic recrystallization, and mechanical properties of Ti–44Al–5Nb–1Mo alloys during direct hot-pack rolling, *Mater. Sci. Eng., A* 773 (2020) 138838.
- [18] H. Clemens, W. Wallgram, S. Kremmer, V. Güther, A. Otto, A. Bartels, Design of novel  $\beta$ -solidifying TiAl alloys with adjustable  $\beta/\beta_2$ -phase fraction and excellent hot-workability, *Adv. Eng. Mater.* 10 (8) (2008) 707–713.

- [19] N. Cui, Q. Wu, Z. Yan, H. Zhou, X. Wang, The microstructural evolution, tensile properties, and phase hardness of a TiAl alloy with a high content of the  $\beta$  phase, *Materials* 12 (17) (2019) 2757.
- [20] H. Fang, R. Chen, X. Chen, Y. Yang, Y. Su, H. Ding, J. Guo, Effect of Ta element on microstructure formation and mechanical properties of high-Nb TiAl alloys, *Intermetallics* 104 (2019) 43–51.
- [21] C. Löffl, H. Saage, M. Göken, In situ X-ray tomography investigation of the crack formation in an intermetallic beta-stabilized TiAl-alloy during a stepwise tensile loading, *Int. J. Fatig.* 124 (2019) 138–148.
- [22] B. Zhu, X. Xue, H. Kou, R. Dong, J. Li, The nucleation of microcracks under tensile stress in multi-phase high Nb-containing TiAl alloys, *Intermetallics* 106 (2019) 13–19.
- [23] T.T. Cheng, M.R. Willis, I.P. Jones, Effects of major alloying additions on the microstructure and mechanical properties of  $\gamma$ -TiAl, *Intermetallics* 7 (1) (1999) 89–99.
- [24] M. Schloffer, B. Rashkova, T. Schöberl, E. Schwaighofer, Z. Zhang, H. Clemens, S. Mayer, Evolution of the  $\omega_0$  phase in a  $\beta$ -stabilized multi-phase TiAl alloy and its effect on hardness, *Acta Mater.* 64 (2014) 241–252.
- [25] L. Song, X. Xu, L. You, Y. Liang, J. Lin, Ordered  $\omega$  phase transformations in Ti-45Al-8.5 Nb-0.2 B alloy, *Intermetallics* 65 (2015) 22–28.
- [26] D. Holec, D. Legut, L. Isaeva, P. Souvatzis, H. Clemens, S. Mayer, Interplay between effect of Mo and chemical disorder on the stability of  $\beta/\beta_0$ -TiAl phase, *Intermetallics* 61 (2015) 85–90.
- [27] D. Huber, R. Werner, H. Clemens, M. Stockinger, Influence of process parameter variation during thermo-mechanical processing of an intermetallic  $\beta$ -stabilized  $\gamma$ -TiAl based alloy, *Mater. Char.* 109 (2015) 116–121.
- [28] B. Jiang, Q. Wang, C. Dong, P.K. Liaw, Exploration of phase structure evolution induced by alloying elements in Ti alloys via a chemical-short-range-order cluster model, *Sci. Rep.* 9 (1) (2019) 1–11.
- [29] S. Tian, H. Jiang, W. Guo, G. Zhang, S. Zeng, Hot deformation, and dynamic recrystallization behavior of TiAl-based alloy, *Intermetallics* 112 (2019) 106521.
- [30] W. Chen, Z. Li, Additive manufacturing of titanium aluminides, in: *Additive Manufacturing for the Aerospace Industry*, Elsevier, 2019, pp. 235–263.
- [31] E. Cakmak, P. Nandwana, D. Shin, Y. Yamamoto, M.N. Gussev, I. Sen, M.H. Seren, T.R. Watkins, J.A. Haynes, A comprehensive study on the fabrication and characterization of Ti-48Al-2Cr-2Nb preforms manufactured using electron beam melting, *Materialia* 6 (2019) 100284.
- [32] L. Song, L. Wang, M. Oehring, X. Hu, F. Appel, U. Lorenz, F. Pyczak, T. Zhang, Evidence for deformation twinning of the D019- $\alpha_2$  phase in a high Nb containing TiAl alloy, *Intermetallics* 109 (2019) 91–96.
- [33] H. Zhu, W. Sun, F. Kong, X. Wang, Z. Song, Y. Chen, Interfacial characteristics and mechanical properties of TiAl/Ti6Al4V laminate composite (LMC) fabricated by vacuum hot pressing, *Mater. Sci. Eng., A* 742 (2019) 704–711.
- [34] M. Cabibbo, Carbon content driven high temperature  $\gamma$ - $\alpha_2$  interface modifications and stability in Ti-46Al-4Nb intermetallic alloy, *Intermetallics* 119 (2020) 106718.
- [35] N. Bibhanshu, A. Bhattacharjee, S. Suwas, Hot deformation response of titanium aluminides Ti-45Al-(5, 10) Nb-0.2 B-0.2 C with pre-conditioned microstructures, *J. Alloys Compd.* (2020) 154584.
- [36] H. Fang, R. Chen, Y. Yang, Y. Su, H. Ding, J. Guo, Effects of tantalum on microstructure evolution and mechanical properties of high-Nb TiAl alloys reinforced by Ti2AlC, *Research* 2019 (2019), 5143179.
- [37] M.J. Blackburn, Some aspects of phase transformations in titanium alloys, in: R.I. Jaffee (Ed.), *Science, Technology, and Application of Titanium*, Oxford Pergamon Press Ltd, Boeing Scientific Research Labs, Seattle, 1970, pp. 633–643.
- [38] A. Knaislová, P. Novák, F. Průša, M. Cabibbo, L. Jaworska, D. Vojtěch, High-temperature oxidation of Ti-Al-Si alloys prepared by powder metallurgy, *J. Alloys Compd.* 810 (2019) 151895.
- [39] H. Hu, X. Wu, R. Wang, W. Li, Q. Liu, Phase stability, mechanical properties and electronic structure of TiAl alloying with W, Mo, Sc and Yb: first-principles study, *J. Alloys Compd.* 658 (2016) 689–696.
- [40] L. Song, F. Appel, L. Wang, M. Oehring, X. Hu, A. Stark, J. He, U. Lorenz, T. Zhang, J. Lin, F. Pyczak, New insights into high-temperature deformation and phase transformation mechanisms of lamellar structures in high Nb-containing TiAl alloys, *Acta Mater.* (2020).
- [41] Y. Chen, H. Kou, L. Cheng, K. Hua, L. Sun, Y. Lu, E. Bouzy, Crystallography of phase transformation during quenching from  $\beta$  phase field of a V-rich TiAl alloy, *J. Mater. Sci.* 54 (2) (2019) 1844–1856.
- [42] K. Zhang, T. Zhang, X. Zhang, L. Song, Corrosion resistance and interfacial morphologies of a high Nb-containing TiAl alloy with and without thermal barrier coatings in molten salts, *Corrosion Sci.* 156 (2019) 139–146.
- [43] Y.K. Kim, S.J. Youn, S.W. Kim, J. Hong, K.A. Lee, High-temperature creep behavior of gamma Ti-48Al-2Cr-2Nb alloy additively manufactured by electron beam melting, *Mater. Sci. Eng.* 763 (2019) 138138.
- [44] L. Zhu, J. Li, B. Tang, Y. Liu, M. Zhang, L. Li, H. Kou, Microstructure evolution and mechanical properties of diffusion bonding high Nb containing TiAl alloy to Ti2AlNb alloy, *Vacuum* 164 (2019) 140–148.
- [45] H. Fang, R. Chen, Y. Liu, Y. Tan, Y. Su, H. Ding, J. Guo, Effects of niobium on phase composition and improving mechanical properties in TiAl alloy reinforced by Ti2AlC, *Intermetallics* 115 (2019) 106630.
- [46] H. Li, Y. Long, X. Liang, Y. Che, Z. Liu, Y. Liu, H. Xu, L. Wang, Effects of multiaxial forging on microstructure and high temperature mechanical properties of powder metallurgy Ti-45Al-7Nb-0.3 W alloy, *Intermetallics* 116 (2020) 106647.
- [47] J. Wang, Q. Luo, H. Wang, Y. Wu, X. Cheng, H. Tang, Microstructure characteristics and failure mechanisms of Ti-48Al-2Nb-2Cr titanium aluminide intermetallic alloy fabricated by directed energy deposition technique, *Additive Manufacturing* 32 (2020) 101007.
- [48] M.R. Mphahlele, E.A. Olevsy, P.A. Olubambi, Spark plasma sintering of near net shape titanium aluminide: a review, in: *Spark Plasma Sintering*, Elsevier, 2019, pp. 281–299.
- [49] J. Beddoes, W. Wallace, L. Zhao, Current understanding of creep behaviour of near  $\gamma$ -titanium aluminides, *Int. Mater. Rev.* 40 (5) (1995) 197–217.
- [50] M.N. Mathabathe, S. Govender, A.S. Bolokang, R.J. Mostert, C.W. Siyisiya, Phase transformation and microstructural control of the  $\alpha$ -solidifying  $\gamma$ -Ti-45Al-2Nb-0.7 Cr-0.3 Si intermetallic alloy, *J. Alloys Compd.* 757 (2018) 8–15.
- [51] M.N. Mathabathe, A.S. Bolokang, G. Govender, R.J. Mostert, C.W. Siyisiya, Structure-property orientation relationship of a  $\gamma/\alpha_2/\text{Ti}_5\text{Si}_3$  in as-cast Ti-45Al-2Nb-0.7 Cr-0.3 Si intermetallic alloy, *J. Alloys Compd.* 765 (2018) 690–699.
- [52] S. Saeedipour, A. Kermanpur, F. Sadeghi, Effect of N addition on microstructure refinement and high temperature mechanical properties of Ti-46Al-8Ta (at.%) intermetallic alloy, *J. Alloys Compd.* 817 (2020) 152749.
- [53] D. Zhang, Y. Chen, G. Zhang, N. Liu, F. Kong, J. Tian, J. Sun, Hot deformation behavior and microstructural evolution of PM Ti43Al9V0.3 with fine equiaxed  $\gamma$  and B2 grain microstructure, *Materials* 13 (4) (2020) 896.
- [54] S. Karthikeyan, G.B. Viswanathan, P.I. Gouma, V.K. Vasudevan, Y.W. Kim, M.J. Mills, Mechanisms, and effect of microstructure on creep of TiAl-based alloys, *Mater. Sci. Eng.* 329 (2002) 621–630.
- [55] P.V. Cobbinah, W. Matizambuka, R. Machaka, M.B. Shongwe, Y. Yamabe-Mitarai, The effect of Ta additions on the oxidation resistance of SPS-produced TiAl alloys, *Int. J. Adv. Manuf. Technol.* 106 (7–8) (2020) 3203–3215.
- [56] H. Huang, H. Ding, X. Xu, The microstructure and mechanical property of TiAl alloy containing  $\beta$ -stabilizer, *Procedia Manufacturing* 37 (2019) 73–79.
- [57] J. Han, Z. Liu, Y. Jia, T. Wang, L. Zhao, J. Guo, S. Xiao, Y. Chen, Effect of TiB2 addition on microstructure and fluidity of cast TiAl alloy, *Vacuum* 174 (2020) 109210.
- [58] P. Sallot, J.P. Monchoux, S. Joulié, A. Couret, M. Thomas, Impact of  $\beta$ -phase in TiAl alloys on mechanical properties after high temperature air exposure, *Intermetallics* 119 (2020) 106729.
- [59] L.H. Ye, H. Wang, G. Zhou, Q.M. Hu, R. Yang, Phase stability of TiAl-X (X = V, Nb, Ta, Cr, Mo, W, and Mn) alloys, *J. Alloys Compd.* 819 (2020) 153291.
- [60] Y. Yang, R.R. Chen, H.Z. Fang, J.J. Guo, H.S. Ding, Y.Q. Su, H.Z. Fu, Improving microstructure and mechanical properties of Ti43Al5Nb0.1B alloy by addition of Fe, *Rare Met.* 38 (11) (2019) 1024–1032.
- [61] G. Yang, X. Yang, Y. Wang, L. Cheng, H. Kou, Y. Liu, Y. Li, P. Wang, W. Ren, Phase precipitation behavior of a quenched  $\beta$ -solidifying TiAl alloy with a fully-B2 microstructure during annealing at 800° C, *J. Alloys Compd.* 812 (2020) 152118.
- [62] Q. Yu, D. Wen, S. Wang, B. Kong, S. Wu, T. Xiao, Effect of 0.8 at.% H on the mechanical properties and microstructure evolution of a Ti-45Al-9Nb alloy under uniaxial tension at high temperature, *Coatings* 10 (1) (2020) 52.
- [63] R. Ding, Y. Chiu, M. Chu, S. Paddea, G. Su, A study of fracture behaviour of gamma lamella using the notched TiAl micro-cantilever, *Phil. Mag.* (2020) 1–16.
- [64] Y. Pan, X. Lu, M.D. Hayat, F. Yang, C. Liu, Y. Li, X. Li, W. Xu, X. Qu, P. Cao, Effect of Sn addition on the high-temperature oxidation behavior of high Nb-containing TiAl alloys, *Corrosion Sci.* (2020) 108449.
- [65] J. Bresler, S. Neumeier, M. Ziener, F. Pyczak, M. Göken, The influence of niobium, tantalum and zirconium on the microstructure and creep strength of fully lamellar  $\gamma/\alpha_2$  titanium aluminides, *Mater. Sci. Eng., A* 744 (2019) 46–53.
- [66] A.V. Bakulin, S.E. Kulkova, Effect of impurities on the formation energy of point defects in the  $\gamma$ -TiAl alloy, *J. Exp. Theor. Phys.* 127 (6) (2018) 1046–1058.
- [67] S.S. Gerstl, Y.W. Kim, D.N. Seidman, Atomic scale chemistry of  $\alpha_2/\gamma$  interfaces in a multi-component TiAl alloy, *Interface Sci.* 12 (2–3) (2004) 303–310.
- [68] G.D. Ren, C.R. Dai, W. Mei, J. Sun, S. Lu, L. Vitos, Formation and temporal evolution of modulated structure in high Nb-containing lamellar  $\gamma$ -TiAl alloy, *Acta Mater.* 165 (2019) 215–227.
- [69] S.J. Qu, S.Q. Tang, A.H. Feng, C. Feng, J. Shen, D.L. Chen, Microstructural evolution, and high-temperature oxidation mechanisms of a titanium aluminide-based alloy, *Acta Mater.* 148 (2018) 300–310.
- [70] W. Lefebvre, A. Menand, A. Loiseau, D. Blavette, Atom probe study of phase transformations in a Ti-48 at. % Al alloy, *Mater. Sci. Eng.* 327 (1) (2002) 40–46.
- [71] F.Y. Hsu, H.J. Klaar, G.X. Wang, M. Dahms, Influence of Si content on microstructure of TiAl alloys, *Mater. Char.* 36 (4–5) (1996) 371–378.
- [72] H.R. Jiang, Z.L. Wang, X.R. Feng, Z.Q. Dong, L. Zhang, L.I.U. Yong, Effects of Nb and Si on high temperature oxidation of TiAl, *Trans. Nonferrous Metals Soc. China* 18 (3) (2008) 512–517.
- [73] G. Baudana, S. Biamino, B. Klöden, A. Kirchner, T. Weißgärber, B. Kieback, M. Pavese, D. Ugues, P. Fino, C. Badini, Electron beam melting of Ti-48Al-2Nb-0.7 Cr-0.3 Si: feasibility investigation, *Intermetallics* 73 (2016) 43–49.
- [74] Y.W. Kim, S.L. Kim, Effects of microstructure and C and Si additions on elevated temperature creep and fatigue of gamma TiAl alloys, *Intermetallics* 53 (2014) 92–101.
- [75] R.C. Pond, P. Shang, T.T. Cheng, M. Aindow, Interfacial dislocation mechanism for diffusional phase transformations exhibiting martensitic crystallography: formation of TiAl+ Ti3Al lamellae, *Acta Mater.* 48 (5) (2000) 1047–1053.
- [76] L. Cha, T. Schmoelzer, Z. Zhang, S. Mayer, H. Clemens, P. Staron, G. Dehm, In situ study of  $\gamma$ -TiAl lamellae formation in supersaturated  $\alpha_2$ -Ti3Al grains, *Adv. Eng. Mater.* 14 (5) (2012) 299–303.
- [77] S.D. Castellanos, A.J. Cavaleiro, A.D. Jesus, R. Neto, J.L. Alves, Machinability of titanium aluminides: a review, in: *The Proceedings of the Institution of Mechanical Engineers, Part L: Journal of Materials: Design and Applications*, 233, 2019, pp. 426–451, 3.



- [78] X. Xu, H. Ding, M. Xing, H. Huang, The microstructure and mechanical property of high niobium TiAl alloy prepared by electromagnetic cold crucible, *Procedia Manufacturing* 37 (2019) 132–137.
- [79] T. Yener, A. Erdogan, M.S. Gök, S. Zeytin, Nb and B effect on mechanical properties of Ti–Al based intermetallic materials, *Vacuum* 169 (2019) 108867.
- [80] K. Zhu, S. Qu, A. Feng, J. Sun, J. Shen, Microstructural evolution and refinement mechanism of a beta–gamma TiAl-based alloy during multidirectional isothermal forging, *Materials* 12 (15) (2019) 2496.
- [81] A. Seidel, S. Saha, T. Maiwald, J. Moritz, S. Polenz, A. Marquardt, J. Kaspar, T. Finaske, E. Lopez, F. Brueckner, C. Leyens, Intrinsic heat treatment within additive manufacturing of gamma titanium aluminide space hardware, *J. Occup. Med.* 71 (4) (2019) 1513–1519.
- [82] T. Schmoelzer, S. Mayer, C. Sailer, F. Haupt, V. Guether, P. Staron, K.D. Liss, H. Clemens, In situ diffraction experiments for the investigation of phase fractions and ordering temperatures in Ti-44 at% Al-(3-7) at% Mo alloys, *Adv. Eng. Mater.* 13 (4) (2011) 306–311.
- [83] H.A. Kishawy, A. Hosseini, Titanium and titanium alloys, in: *Machining Difficult-To-Cut Materials*, Springer, Cham, 2019, pp. 55–96.
- [84] D. Wimler, J. Lindemann, H. Clemens, S. Mayer, Microstructural evolution and mechanical properties of an advanced  $\gamma$ -TiAl based alloy processed by spark plasma sintering, *Materials* 12 (9) (2019) 1523.
- [85] J. Wang, Z. Pan, D. Cuiuri, H. Li, Phase constituent control and correlated properties of titanium aluminide intermetallic alloys through dual-wire arc additive manufacturing, *Mater. Lett.* 242 (2019) 111–114.
- [86] S. Yuke, S.W. Kim, J. Hahn, D.B. Lee, High-temperature corrosion of Ti-46Al-6Nb-0.5 W-0.5 Cr-0.3 Si-0.1 C alloy in N<sub>2</sub>/0.1% H<sub>2</sub> S gas, *Oxid. Metals* 91 (5-6) (2019) 677–689.
- [87] R. Swadzba, L. Swadzba, B. Mendala, B. Witala, J. Tracz, K. Marugi, Characterization of Si-aluminide coating and oxide scale microstructure formed on  $\gamma$ -TiAl alloy during long-term oxidation at 950° C, *Intermetallics* 87 (2017) 81–89.
- [88] M. Oehring, A. Stark, J.D. Paul, T. Lippmann, F. Pyczak, Microstructural refinement of boron containing  $\beta$ -solidifying  $\gamma$ -titanium aluminide alloys, *Mater. Sci. Forum* 706 (2012) 1089–1094.
- [89] J. Liu, F. Zhang, H. Nan, X. Feng, X. Ding, Effect of C Addition on as-cast microstructures of high Nb containing TiAl alloys, *Metals* 9 (11) (2019) 1201.
- [90] R.R. Xu, H. Li, M.Q. Li, Flow softening mechanism in isothermal compression of  $\beta$ -solidifying  $\gamma$ -TiAl alloy, *Mater. Des.* 186 (2020) 108328.
- [91] J. Yang, B. Cao, Y. Wu, Z. Gao, R. Hu, Continuous cooling transformation (CCT) behavior of a high Nb-containing TiAl alloy, *Materialia* 5 (2019) 100169.
- [92] L. Mengis, C. Grimme, M.C. Galezit, High-temperature sliding wear behavior of an intermetallic  $\gamma$ -based TiAl alloy, *Wear* 426 (2019) 341–347.
- [93] J. Qiu, Z. Fu, B. Liu, Y. Liu, J. Yan, D. Pan, W. Zhang, I. Baker, Effects of niobium particles on the wear behavior of powder metallurgical  $\gamma$ -TiAl alloy in different environments, *Wear* 434 (2019) 202964.
- [94] N.S. Neelam, S. Banumathy, A. Bhattacharjee, G.V.S. NageswaraRao, The effect of Cr and Mo addition on the oxidation behaviour of Ti-46.5 Al-3.5 Nb-2Cr-0.3 B, *Mater. Today: Proceedings* 15 (2019) 30–35.
- [95] P.V. Panin, N.A. Nozhovnaya, E.A. Lukina, A.S. Kochetkov, Effect of chemical composition variability on phase composition and structure of beta-solidifying TiAl-alloy in as-cast condition, *inorganic materials*, *Applied Research* 10 (2) (2019) 316–321.
- [96] R. Kainuma, Y. Fujita, H. Mitsui, I. Ohnuma, K. Ishida, Phase equilibria among  $\alpha$ (hcp),  $\beta$ (bcc) and  $\gamma$ (L10) phases in Ti–Al base ternary alloys, *Intermetallics* 8 (8) (2000) 855–867.
- [97] L. Song, X.J. Xu, L. You, Y.F. Liang, J.P. Lin, Phase transformation and decomposition mechanisms of the  $\beta_0$  ( $\omega$ ) phase in cast high Nb containing TiAl alloy, *J. Alloys Compd.* 616 (2014) 483–491.
- [98] Y. Lu, J. Yamada, R. Miyata, H. Kato, K. Yoshimi, High-temperature mechanical behavior of B2-ordered Ti–Mo–Al alloys, *Intermetallics* 117 (2020) 106675.
- [99] Q. Wang, R. Chen, Y. Yang, J. Guo, Y. Su, H. Ding, H. Fu, Improvement of the creep lifetimes and microstructural stability of  $\beta$ -solidifying  $\gamma$ -TiAl by cold crucible directional solidification, *Intermetallics* 100 (2018) 104–111.
- [100] T. Klein, D. Holec, H. Clemens, S. Mayer, Pathways of phase transformation in  $\beta$ -phase-stabilized  $\sigma/\gamma$ -TiAl alloys subjected to two-step heat treatments, *Scripta Mater.* 149 (2018) 70–74.
- [101] P.L. Narayana, C.L. Li, S.W. Kim, S.E. Kim, A. Marquardt, C. Leyens, N.S. Reddy, J.T. Yeom, J.K. Hong, High strength and ductility of electron beam melted  $\beta$  stabilized  $\gamma$ -TiAl alloy at 800° C, *Mater. Sci. Eng.* 756 (2019) 41–45.
- [102] J.A. Stendal, M. Eisentraut, I. Sizova, S. Bolz, M. Bambach, S. Weiß, Effect of heat treatment on the workability of hot isostatically pressed TNM-B1, in: *AIP Conference Proceedings*, 2113, AIP Publishing LLC, 2019, July, p. 40010, 1.
- [103] V.M. Tabie, C. Li, W. Saifu, J. Li, X. Xu, Mechanical properties of near alpha titanium alloys for high-temperature applications-a review, *Aircraft Eng. Aero. Technol.* (2020).
- [104] V.E. Bazhenov, V.S. Kuprienko, A.V. Fadeev, A.I. Bazlov, V.D. Belov, A.Y. Titov, A.V. Kolytgin, A.A. Komissarov, I.V. Plisetskaya, I.A. Logachev, Influence of Y and Zr on TiAl43Nb4Mo1B0. 1 titanium aluminide microstructure and properties, *Mater. Sci. Technol.* 36 (5) (2020) 548–555.
- [105] K. Zhang, R. Hu, T. Lei, J. Yang, Refinement of massive  $\gamma$  phase with enhanced properties in a Ta containing  $\gamma$ -TiAl-based alloys, *Scripta Mater.* 172 (2019) 113–118.
- [106] V. Singh, C. Mondal, A. Kumar, P.P. Bhattacharjee, P. Ghosal, High temperature compressive flow behavior and associated microstructural development in a  $\beta$ -stabilized high Nb-containing  $\gamma$ -TiAl based alloy, *J. Alloys Compd.* 788 (2019) 573–585.
- [107] Q. Wu, N. Cui, X. Xiao, X. Wang, E. Zhao, Hot deformation behavior and microstructural evolution of a novel  $\beta$ -solidifying Ti–43Al–3Mn–2Nb–0.1 Y alloy, *Materials* 12 (13) (2019) 2172.
- [108] T.B. Ershova, N.M. Vlasova, I.A. Astapov, M.A. Teslina, Carbaborating of the intermetallic Ti 3 Al-based alloys, *Inorg. Mater.: Applied Research* 10 (1) (2019) 1–4.
- [109] L. Song, L. Wang, T. Zhang, J. Lin, F. Pyczak, Microstructure and phase transformations of  $\omega$ -Ti4Al3Nb based alloys after quenching and subsequent aging at intermediate temperatures, *J. Alloys Compd.* 821 (2020) 153387.
- [110] E. Schwaighofer, B. Rashkova, H. Clemens, A. Stark, S. Mayer, Effect of carbon addition on solidification behaviour, phase evolution and creep property of an intermetallic  $\beta$ -stabilized  $\gamma$ -TiAl based alloy, *Intermetallics* 46 (2014) 173–184.
- [111] L. Song, X. Hu, L. Wang, A. Stark, D. Lazurenko, U. Lorenz, J. Lin, F. Pyczak, T. Zhang, Microstructure evolution and enhanced creep property of a high Nb containing TiAl alloy with carbon addition, *J. Alloys Compd.* 807 (2019) 151649.
- [112] S. Karthikeyan, M.J. Mills, The role of microstructural stability on compression creep of fully lamellar  $\gamma$ -TiAl alloys, *Intermetallics* 13 (9) (2005) 985–992.
- [113] F.S. Sun, F.S. Froes, Precipitation of Ti5Si3 phase in TiAl alloys, *Mater. Sci. Eng.* 328 (1-2) (2002) 113–121.
- [114] J.H. Lee, H.K. Park, J.H. Kim, J.H. Jang, S.K. Hong, I.H. Oh, Constitutive behavior and microstructural evolution in Ti–Al–Si ternary alloys processed by mechanical milling and spark plasma sintering, *Journal of Materials Research and Technology* (2020).
- [115] A. Knaislová, J. Linhart, P. Novák, F. Průša, J. Kopeček, F. Laufek, D. Vojtěch, Preparation of TiAl15Si15 intermetallic alloy by mechanical alloying and the spark plasma sintering method, *Powder Metall.* 62 (1) (2019) 54–60.
- [116] X.W. Du, J.N. Wang, J. Zhu, The influence of Si alloying on the creep microstructure and property of a TiAl alloy prepared by powder metallurgy, *Intermetallics* 9 (9) (2001) 745–753.
- [117] A. Knaislová, P. Novák, J. Kopeček, F. Průša, Properties comparison of Ti–Al–Si alloys produced by various metallurgy methods, *Materials* 12 (19) (2019) 3084.
- [118] S. Nouri, S. Sahmani, M. Asayesh, M.M. Aghdam, Study on the oxidation resistance of  $\gamma$ -TiAl intermetallic alloy coated via different diffusion coating processes, *Mater. Res. Express* 6 (10) (2019) 106522.
- [119] M.K. Yadav, A.N. Siddiquee, Z.A. Khan, Characterization of Ti–Al intermetallic synthesized by mechanical alloying process, *Met. Mater. Int.* (2020) 1–9.
- [120] M.D. Hayat, H. Singh, Z. He, P. Cao, Titanium metal matrix composites: an overview, *Composites Part A* 121 (2019) 418–438.
- [121] Y. Wu, S. Zhang, X. Cheng, H. Wang, Investigation on solid-state phase transformation in a Ti-47Al-2Cr-2V alloy due to thermal cycling during laser additive manufacturing process, *J. Alloys Compd.* 799 (2019) 325–333.
- [122] W. Kan, B. Chen, H. Peng, Y. Liang, J. Lin, Formation of columnar lamellar colony grain structure in a high Nb-TiAl alloy by electron beam melting, *J. Alloys Compd.* 809 (2019) 151673.
- [123] M. Tlotleng, S. Pityana, Effects of Al and heat treatment on the microstructure and hardness of Ti–Al synthesized via in situ melting using LENS, *Metals* 9 (6) (2019) 623.
- [124] Y. Lu, J. Yamada, R. Miyata, H. Kato, K. Yoshimi, High-temperature mechanical behavior of B2-ordered Ti–Mo–Al alloys, *Intermetallics* 117 (2020) 106675.